Plant Physiology and Biochemistry 229 (2025) 110325

Contents lists available at ScienceDirect

Plant Physiology and Biochemistry

journal homepage: www.elsevier.com/locate/plaphy

Reproductive stage-dependent heat stress responses from perspectives of photosynthesis, yield, and grain composition in contrasting *Lupinus angustifolius* varieties

Mikuláš Kňazovický [a,*], Eva Rosenqvist [b], Oriane Bouché [a], Rong Zhou [c], Carl-Otto Ottosen [a]

[a] Department of Food Science, Plant, Food & Climate, Aarhus University, Agro Food Park 48, Aarhus N, DK-8200, Denmark
[b] Department of Plant and Environmental Sciences, Crop Sciences, University of Copenhagen, Hoejbakkegaard Allé 9, Taastrup, DK-2630, Denmark
[c] Sanya Institute of Nanjing Agricultural University, Nanjing Agricultural University, Jiangsu, Nanjing, 210095, China

ARTICLE INFO

Keywords:
Climate change
Abiotic stress
Thermal tolerance
Lupinus angustifolius
Gas exchange
Chlorophyll fluorescence
Grain protein

ABSTRACT

This study aimed to elucidate heat resistance in *Lupinus angustifolius* L. using gas exchange and chlorophyll fluorescence methods and to examine relationships between photosynthesis, yield, and grain nutritional composition. For this we exploited six contrasting varieties: 'Iris', 'Jenabillup', 'Mandelup', 'Mirabor', 'Primabella' and 'Primadonna' selected based on physiological, yield, and grain nutritional performance. Plants were subjected to three day/night temperature regimes (23/18 °C, 30/25 °C, and 38/33 °C) for five days during one of two reproductive stages: flower spike emergence and grain filling. At the flower spike emergence, the 38/33 °C decreased the photosynthetic CO_2 assimilation (A_n) in all varieties, with notable differences observed among them. 'Mandelup', 'Iris', and 'Jenabillup' maintained the highest A_n. At grain filling, the effects of 38/33 °C were more pronounced, resulting in a greater reduction in A_n. Notably, 'Primabella' and 'Primadonna' exhibited the most substantial decrease in A_n. The investigation of chlorophyll quenching parameters revealed significant impacts of temperature treatments on the maximum quantum efficiency of PSII (F_v/F_m), with notable varietal distinctions particularly during the grain filling stage. We found strong correlations between photosynthetic parameters and yield traits, as well as grain nutritional composition. These relationships were also strongly dependent on stage of development at which the heat stress was imposed, which underlines the critical importance of timing in phenotyping. Our findings provide a foundation for future molecular, metabolomic, and physiological studies on heat tolerance in lupins and promote adoption of heat-tolerant varieties in European cropping systems in the face of worsening effects of climate change and increased demand for plant protein.

1. Introduction

Climate change, accompanied by increasing frequency of heatwaves, poses a significant challenge to the global crop production. Heat stress is a major contributor to yield losses (Fahad et al., 2017; Zhongming et al., 2022). This exacerbates global food insecurity, currently affecting more than 820 million people (Willett et al., 2019), and the situation is expected to worsen as the average global temperature rises (Zhongming

Abbreviations: $\mathbf{A_{max}}$, maximum net assimilation rate at light saturation; $\mathbf{A_n}$, net CO_2 assimilation rate; $\mathbf{A_n/C_i}$, intercellular CO_2 response curve of photosynthesis; $\mathbf{A_n/Q}$, light response curve; $\mathbf{C_a}$, atmospheric CO_2 concentration; **E**, transpiration rates; **ETR**, electron transport rate; $\mathbf{F_v/F_m}$, maximum quantum efficiency of PSII; $\mathbf{g_s}$, stomatal conductance; $\mathbf{J_{max}}$, maximum RuBP regeneration rate; **LCP**, light compensation point; **NPQ**, non-photochemical fluorescence quenching; **PETC**, photosynthetic electron transport chain; **PPFD**, photosynthetic photon flux density; $\mathbf{P_r}$, photorespiration rate; $\mathbf{q_L}$, fraction of open PSII centres; $\mathbf{q_N}$, coefficient of non-photochemical fluorescence quenching; $\mathbf{q_P}$, coefficient of photochemical fluorescence quenching; **Rca**, Rubisco activase; $\mathbf{R_d}$, dark respiration rate; **RH**, relative humidity; **ROS**, reactive oxygen species; **TGW**, thousand grain weight; $\mathbf{V_{cmax}}$, maximum rate of carboxylation; **VPD**, vapor pressure deficit; $\mathbf{WUE_i}$, intrinsic water use efficiency; $\mathbf{WUE_{leaf}}$, Instantaneous water use efficiency; **Y-NO**, quantum yield of non-photochemical energy conversion in PSII other than that caused by down-regulation of the light-harvesting function; **Y-NPQ**, quantum yield of non-photochemical energy conversion in PSII due to down-regulation of the light-harvesting function; $\mathbf{Y_{Carb}}$, carbohydrate yield; $\mathbf{Y_{Prot}}$, protein yield; α, apparent quantum yield of CO_2 assimilation; **θ**, curve convexity; **ΔT**, leaf cooling.

* Corresponding author.
E-mail address: mikulaskn@food.au.dk (M. Kňazovický).

https://doi.org/10.1016/j.plaphy.2025.110325
Received 17 March 2025; Received in revised form 28 July 2025; Accepted 31 July 2025
Available online 9 August 2025

et al., 2022).

Legumes, known for their high grain protein content (Bennetau-Pelissero, 2019), are considered a cornerstone of sustainable diets (Willett et al., 2019; Ferreira et al., 2021). However, despite European yields being among the world's highest (Lucas et al., 2015), *Lupinus* spp. have until now made only minor contributions to the total European legume yields due to their limited cropping area. In recent times, lupins have gained increased attention because of their high protein (30–44 %) and essential amino acids content (Frick et al., 2018; Bennetau-Pelissero, 2019; Sarkar et al., 2021), as well as advancement of varieties with restricted branching allowing for a more uniform yield (Vishnyakova et al., 2021). As a comparison, the protein content reaches 8–10 % in rice, 8–20 % in wheat, and 40–41 % in the currently dominating protein crop – soybean (Chen et al., 2023; Zhang et al., 2024). As lupins can obtain atmospheric nitrogen through *Rhizobium* bacteria, thereby reducing the reliance on inorganic fertilizers and promoting soil fertility, they are crucial for sustainable agriculture and reducing the greenhouse gas emissions from agriculture (Zhongming et al., 2022).

One of the earliest biochemical limitations to carbon assimilation during heat stress is the reduced activation of Rubisco, the key CO_2-fixing enzyme, due to impaired function of its activator, Rubisco activase (Rca) (Crafts-Brandner and Law, 2000; Scafaro et al., 2023). Elevated temperatures also decrease the CO_2 specificity of Rubisco and alter the $O_{2/CO2}$ solubility ratio within the cell, which enhances the enzyme's oxygenase activity and thereby increases photorespiration (Jordan and Ogren, 1984; Dusenge et al., 2019). This downregulation of Rubisco activity can, in turn, limit the regeneration of $NADP^+$, the terminal electron acceptor in the photosynthetic electron transport chain (PETC), leading to its over-reduction (Moore et al., 2021; de Souza et al., 2024). As a result, less absorbed light energy is used for carbon fixation, so excess excitation energy accumulates. To dissipate this excess energy under stress, plants typically enhance non-photochemical quenching (NPQ) mechanisms (Chauhan et al., 2023). However, high excitation pressure may still cause oxidative damage to nearby membranes, pigments, and proteins such as the D1 protein of photosystem II (PSII), resulting in PSII inactivation (Ahammed et al., 2018). Furthermore, when the PETC becomes overly reduced—particularly due to accumulation of reduced plastoquinone—charge recombination in PSII may lead to the formation of singlet oxygen, a highly reactive species that exacerbates oxidative stress (Mathur et al., 2014). The imbalance between reactive oxygen species (ROS) generation and detoxification disrupts thylakoid membrane integrity, hampers D1 repair, and reduces photosynthetic efficiency parameters such as electron transport rate (ETR), PSII maximum quantum efficiency (F_v/F_m), and the proportion of open PSII centres (q_L) (Demidchik, 2015; Murchie and Lawson, 2013; Ahammed et al., 2018). Moreover, because ATP synthesis depends on the proton gradient across the thylakoid membrane, any reduction in ETR directly limits ATP production.

Heat-tolerance, defined as the ability to produce economic yield under supraoptimal temperatures (Sato et al., 2024), is critical for future food security. Physiological phenotyping for climate stress tolerance is an established method for identifying and describing climate-resistant varieties (Abdelhakim et al., 2022b; Moore et al., 2021; Rosenqvist, 2022). Yet, phenotyping studies are often constrained by a lack of integration with yield-related traits and grain quality metrics, which are essential for translating stress responses into meaningful outcomes for crop production. Improved knowledge on heat resistance and its underpinning mechanisms, particularly how these relate to yield performance and grain nutritional composition in lupins, could promote its use in European cropping systems as the climate stresses intensify. Plants can acclimate to elevated temperatures through intricate resistance mechanisms. Under heat stress conditions with adequate water supply, the transpiration (E), controlled by the stomata, plays a key role in varietal response. Varieties with high E can substantially reduce leaf temperature, allowing the photosynthetic apparatus to operate closer to its temperature optimum as opposed to varieties with lower transpiration rates. Therefore, the ability of the different varieties to sustain high leaf cooling (ΔT) under heat stress can serve as one of key traits for distinguishing heat-tolerant and heat-sensitive varieties in both leguminous and non-leguminous crops. (Mahalingam, 2014). For example, heat resistant common bean cultivars showed high stomatal conductance (g_s) and leaf cooling in response to elevated temperatures (Deva et al., 2020). In non-leguminous crops, Poudyal et al. (2018) measured the F_v/F_m response of 28 tomato genotypes to heat stress and found a significant genotypic variability, with the resistant varieties also showing stronger stomatal response, leaf cooling, CO_2 assimilation rate (A_n), and maintaining the yield under field conditions with natural heat wave, underlining the robustness of this methodology (Poudyal et al., 2018; Sharma et al., 2015). Zhou et al. (2018) used F_v/F_m measurements in phenotyping 127 faba bean varieties, successfully distinguishing between resistant and sensitive lines. Ibrahim (2011) measured the membrane thermostability and canopy temperature of 45 chickpea, lentil, and faba bean genotypes grown in the field, with both parameters showing significant genotypic variability. Thus, various physiological parameters can be employed in search for heat stress resistance across a diverse range of plants.

In this study, we selected six *L. angustifolius* varieties based on prior screening for contrasting physiological responses to heat stress and grain nutritional characteristics. These included differences in PSII efficiency, grain protein content, and quinolizidine alkaloid levels, as well as geographic origin, with both Australian and European lines represented. This study's objective is to derive better understanding of lupin's physiological response to heat stress and elucidate its resistance mechanisms through a combination of gas exchange and chlorophyll fluorescence methodologies. Additionally, we aim to investigate how heat stress during specific reproductive stages influences both photosynthetic physiology, grain yield components, and the grain nutritional composition. This leads us to our primary hypothesis, that heat tolerant varieties will maintain higher levels of photosynthetic parameters, such as A_n and F_v/F_m. We hypothesize, that ΔT plays a key role in maintenance of said parameters. Lastly, we expect significant positive relationships of the photosynthetic parameters with yield related parameters. Illumination of these relationships will contribute to development of robust interdisciplinary heat-stress tolerance screening protocols for this crop. Notably, this study represents the first comprehensive physiological examination of varietal performance under varying stages of development in response to heat stress for this species.

2. Materials & methods

2.1. Plant material and cultivation environment

Based on previous pilot studies, six varieties of *L. angustifolius* with normal and restricted branching patterns were selected, including: 'Iris', 'Jenabillup', 'Mandelup', 'Mirabor', 'Primabella' and 'Primadonna'. A preliminary heat stress screening of 25 varieties revealed that 'Mirabor' and 'Iris' maintained the highest PSII efficiency (F_v/F_m), whereas 'Primadonna' exhibited the lowest. Furthermore, the results from Roman et al. (2023) indicate high protein content in both 'Mirabor' and 'Primadonna', but substantial differences in quinolizidine alkaloid content. The geographic origin of the varieties, with 'Jenabillup' and 'Mandelup' sourced from Australia and the rest from Europe, was also considered to ensure broader representation. Four seeds were sown in 3 L pots filled with peat substrate (Pinstrup 2, Pindstrup Mosebrug, Ryomgaard, Denmark), with six pots per variety and treatment. To facilitate nodulation each seed was coated with LEGUMEFIX (LEGUME technology, Nottinghamshire, United Kingdom) before sowing. The plants were grown in a greenhouse at Aarhus University, Department of Food Science, with temperature settings 20/18 °C (day/night), 50 % relative humidity (RH), daily irrigation with full nutrient solution (pH = 6.3; EC = 2.86 mS cm^{-1}), 16-h photoperiod, with natural light supplemented by LED lamps (FL300 Grow, Senmatic, Søndersø, Denmark) when the

photosynthetic photon flux density (PPFD) decreased bellow 150 μmol m^{-2} s^{-1}. The greenhouse climate was regulated with LCC4 (Senmatic A/S, Søndersø, Denmark) based on inputs from a thermometer (PT100, RS Pro, GB), a humidity sensor (HMP60, Vaisala, Finland), and a quantum sensor (Li-Cor, United Kingdom). After three weeks, one plant per pot was selected and kept and finally, from the six pots, four were used as experimental replicates. This selection procedure was based on experience with a frequent abnormal plant development during the pilot studies.

2.2. Temperature treatments and stages of reproductive development

Plants were exposed to three temperature treatments: 23/18 °C (CT23; VPD 1.3/0.9 kPa), 30/25 °C (HS30; VPD 2.4/1.7 kPa), 38/33 °C (HS38; VPD 3.7/2.7 kPa), for five days during one of two reproductive stages of development: flower spike emergence (early reproductive development), and grain filling (late reproductive development). Each temperature treatment was simulated in a separate climate chamber (Photon System Instruments, Drásov, Czech Republic). Plants were irrigated daily with a full nutrient solution, PPFD was maintained at 300 μmol m^{-2} s^{-1}, and photoperiod at 16 h. The transition from night to day temperatures was achieved with a 1-h temperature ramp beginning at 06:00. This was followed by 14 h at a steady treatment temperature, after which another 1-h ramp facilitated the transition back to night temperatures. Before the start of each temperature treatment, the plants were placed in a control chamber for a two-day acclimation period and subsequently transferred into another chamber with a corresponding temperature treatment and randomized. The measurements and tissue collection for further analyses were conducted on the last day of treatment.

2.3. Gas exchange measurements

The gas exchange measurements were conducted on biological replicates from control and heat stress treatments, using a portable gas exchange and fluorescence system GFS-3000 with an integrated LED array and PAM-Fluorometer 3056-FL (Walz, Effeltrich, Germany). The light response curve (A_n/Q) was constructed by reaching a steady state of A_n at a set of PPFD levels, as defined in Rosenqvist (2022), starting at 1000 μmol m^{-2} s^{-1}. During the A_n/Q curve, the atmospheric CO_2 concentration (C_a) was maintained at 400 ppm. The intercellular CO_2 response curve of photosynthesis (A_n/C_i) was designed to reach a steady state of A_n at a set of CO_2 levels, as defined in Rosenqvist (2022), starting at 400 ppm. The PPFD was maintained at 1500 μmol m^{-2} s^{-1} throughout the A_n/C_i response. A_n/Q and A_n/C_i curves were measured on 12–16 and 10–16 biological replicates, respectively, with snapshots at 1500 μmol m^{-2} s^{-1} PPFD extracted from the A_n/Q curves for comparison. During both A_n/Q, and A_n/C_i curve measurements, the cuvette temperature and RH was set according to treatment: for CT23, the cuvette temperature was set to 23 °C (55 % RH, VPD = 14.9 ± 0.13 Pa/kPa), for HS30 to 30 °C (45 % RH, VPD = 20.4 ± 0.19 Pa/kPa), and for HS38 to 38 °C (45 % RH, VPD = 29.4 ± 0.48 Pa/kPa). During the measurements of heat stressed plants, the room temperature was increased to 30 °C, and a heat cable was used to prevent water condensation in the cuvette tubing. The following parameters were derived from A_n/Q and A_n/C_i curves with the functionality from photosynthesis (version 2.1.4) and plantecophys (version 1.4–6) R packages (version 4.2.2, R Core Team, Vienna, Austria): maximum net assimilation rate at light saturation (A_{max}), apparent quantum yield of CO_2 assimilation (α), dark respiration rate (R_d), light compensation point (LCP), curve convexity (θ), maximum rate of carboxylation (V_{cmax}), and maximum RuBP regeneration rate (J_{max}). Instantaneous (WUE_{leaf}) and intrinsic water use efficiency (WUE_i) was calculated by dividing A_n by g_s, and E, respectively, at PPFD 1500 μmol m^{-2} s^{-1} (Hatfield and Dold, 2019). The photorespiration rate (P_r) was estimated for all treatments according to Valentini et al. (1995) and de Souza et al. (2024) as:

$$P_r = 1/12[ETR - 4(A_n + R_d/2)].$$

The ΔT was calculated with the equation

$$\Delta T = T_{leaf} - T_{cuv},$$

where T_{leaf} is the leaf temperature, T_{cuv} the cuvette temperature, and negative values indicate leaf cooling.

A 2.4 cm^2 leaf area adapter was used; however, the area of each measured leaflet section was individually determined for each replicate. This procedure was put in place due to the leaflet area always falling below the lowest available GFS cuvette area. This determination was made through a custom-made MATLAB (R2022B) image segmentation script and a standardized leaf imaging-station. More details on the validation method are provided in the Supplementary Materials section (Table S. 5).

2.4. Chlorophyll fluorescence quenching

Chlorophyll *a* fluorescence quenching parameters were determined using a Portable Chlorophyll Fluorometer PAM-2500 (Walz, Effeltrich, Germany), and an automated protocol optimized for lupins in the PamWin-3 software. In total 14–16 biological replicates were measured. Following parameters were quantified: effective photochemical quantum yield of PSII (F_q'/F_m'), quantum yield of non-photochemical energy conversion in PSII due to down-regulation of the light-harvesting function (Y-NPQ), quantum yield of non-photochemical energy conversion in PSII other than that caused by down-regulation of the light-harvesting function (Y-NO), non-photochemical fluorescence quenching (NPQ), coefficient of non-photochemical fluorescence quenching (q_N), coefficient of photochemical fluorescence quenching (q_P), fraction of open PSII centres (q_L), ETR, and F_v/F_m (Maxwell and Johnson, 2000; Murchie and Lawson, 2013).

2.5. Yield components

Upon senescence, pods from all individual replicates were harvested separately and later pooled according to the corresponding batches. The batch from each treatment combination contained 3–4 biological replicates. With a total of four batches for each individual treatment, the final pooled replicate count per treatment was four. Pooling was done to enable standardized processing using an automated image analysis platform, while also reducing the labour required for individually handling large numbers of plants. The pooled samples were analysed separately for TGW, grain count, and yield using an automated image segmentation MARViN ProLine platform (MARViTECH, Wittenburg, Germany). Parameters grain count and grain yield were standardized according to the number of biological replicates per pooled sample.

2.6. Proximal nutritional analysis

The nutritional composition of the pooled grain samples collected from plants treated at grain filling was further analysed ($n = 4$). Before milling, grains were dried in a freeze-dryer for a period of three days, followed by milling at a size of 500 μm using a Miller at a speed of 6000 rpm. The powder was collected and stored at 4 °C.

The nitrogen content of the powders was determined using the dumas combustion analysis method with the equipment DUMATHERM (Gerhardt, Königswinter, Germany). All samples were prepared by weighing 15 mg of powder in DumaFoil and recording the exact weight. A nitrogen to protein conversion factor of 5.7 was applied. Tris (hydroxymethyl)aminomethane (THAM) was used as a standard for calibration.

A Folch procedure adapted from Keuleyan et al. (2023), was carried out to perform the lipid extraction. 100 mg of powder was hydrated in 600 μL phosphate buffer (pH 7, 0.01 M) overnight at 4 °C under

magnetic stirring. The precise weight of powder was recorded (P0). The next morning, 5 mL of chloroform/methanol extraction solvent (2:1 v/v) were added to the hydrated powders. After stirring the mixture for 1 h, a filtration under vacuum to retrieve the liquid phase was performed. To limit the loss of products, the powder was washed with 4 mL of extraction solvent and filtrated again. This procedure was repeated twice. The obtained filtrate was then transferred into a tube with 3.5 mL of NaCl (0.73 % w/v), mixed, and centrifuged at 4 °C, 1000 g for 10 min. The bottom organic phase was then collected in small beakers using Pasteur pipettes. After addition of anhydrous sodium sulphate and vacuum filtration, the filtrate was recovered in an empty weighed glass tube (W0) and the solvent was evaporated under Speed vacuum evaporator Genevac EZ-2 Elite (Genevac Ltd, Ipswich, UK) at 38 °C. The glass tubes were then weighed once they were at room temperature (W1). The lipids contents were then quantified by the following formula:

$$Amount\ of\ lipid\ (\%) = \frac{100 \times (W_1 - W_0)}{P_0}$$

Moisture and ashes were quantified using a muffle furnace (Nabertherm GmbH, Bremen, Germany). About 1 g of powder was weighed in porcelain crucible and dried at 105 °C for 3 h. Subsequently the crucibles were weighed, then put in a muffle furnace for 30 min and weighted again. The procedure was repeated until the weigh obtained was constant between two measurements. The dry powder was then let to carbonize at 550 °C for 5 h. The determination of ash content was done after weighing the remaining minerals left in the crucible after cooling down. For quantification of ash and moisture content see Supplementary Materials. After the quantification of proteins, lipids, moisture and minerals, the remaining percentage left in the powder to reach 100 % was considered as carbohydrate.

Lastly, protein and carbohydrate yields were calculated according to the following equation:

$$Y_{component} = Y_{grain} \times C_{component}$$

where:

- $Y_{component}$ = Yield of the specific grain nutritional component (protein, carbohydrate) per plant (g).
- Y_{plant} = Total grain yield per plant (g).
- $C_{component}$ = Content of the specific component in the grain (g per g of grain powder), representing its proportion in the grain mass.

2.6.1. Statistical analysis

All analyses were conducted in RStudio (R version 4.2.2). Prior to ANOVA, assumptions of normality and homoscedasticity were assessed. Parameters including A_n, A_{max}, R_d, grain yield, grain count, TGW, protein, carbohydrates, lipids, ash, and moisture met these assumptions and were analysed using Gaussian models.

Parameters such as E, C_i, ETR, LCP, J_{max}, V_{cmax}, TGW, grain count, and yield were analysed using Gamma models (due to assumptions of normality and homoscedasticity not being met). Distribution fit was confirmed using internal R diagnostics. One-, two-, and three-way ANOVA was applied as appropriate.

Traits not meeting parametric assumptions (ΔT, g_s, P_r, F_v/F_m, NPQ, and q_L) were analysed using the Kruskal–Wallis test via the kruskal() function from the *agricolae* package (v1.3-7). *Post-hoc* tests for parametric and Gamma-distributed variables were performed with posthoc() from the *postHoc* package (v0.1.3).

Principal component analysis (PCA) was performed on batch-averaged data (variety × temperature × developmental stage), including physiological traits, yield components, and grain nutritional parameters. Data were centred and scaled using scale(), and PCA was conducted with prcomp() and visualized using autoplot() from *ggplot2* (v3.5.1). Pairwise correlations among selected traits within each temperature treatment and stage (flowering, grain filling) were computed with cor() and visualized using corrplot() (*corrplot* v0.95). Significance was tested with cor.mtest() ($\alpha < 0.05$).

3. Results

3.1. Developmental stage modifies varietal CO_2 assimilation response to severe heat stress

As expected, temperature treatments showed strong effect on A_n ($p < 0.0001$). During flower spike emergence, HS30 had limited impact on A_n compared to control (CT23), except for 'Primabella', which showed a significant reduction (−12 %; Fig. 1A). As anticipated, HS38 reduced A_n in all varieties, with notable differences observed among them ($p < 0.0001$). 'Mandelup', 'Iris', and 'Jenabillup', maintained a significantly higher A_n relative to 'Mirabor' and 'Primadonna' (Fig. 1A and Table S1). These responses were significantly modified by the stage of development ($p < 0.0001$).

During grain filling, the effect of HS38 was more pronounced, resulting in a greater reduction in A_n in all varieties compared to flower spike emergence. Notably, 'Primabella' and 'Primadonna' showed the most substantial decrease in A_n (56 % and 62 %, respectively), contrasting with the relatively better performance of 'Mirabor', 'Iris', and 'Jenabillup' (Fig. 1A and Table S1). The reduction of A_n in response to HS38 was mirrored by a significant increase in C_i. While no notable differences in C_i between varieties were detected at flower spike emergence, significant variability was observed across all temperature treatments during grain filling (Table S1). 'Primabella' and 'Primadonna' showed the highest C_i values in all temperature treatments, while the lowest values were consistently recorded for 'Mirabor', 'Iris', and 'Jenabillup' (Figs. 1B, 2A and 2B).

3.2. The stomatal response to severe heat stress is dependent on developmental stage

There was a notable difference in the stomatal response to the temperature treatments between the two developmental stages ($p < 0.0001$; Fig. 1C). During flower spike emergence, the g_s was unaffected under HS30, but increased sharply in response to the HS38 (47 % on average). However, this response was nearly absent at grain filling. While 'Mirabor' and 'Primadonna' exhibited a limited yet significant increase in g_s in response to both HS30 and HS38 relative to CT23, no significant changes were detected in the other tested varieties (Fig. 1C). Given the close relationship with g_s, similar patterns were observed in E, with a slight increase in response to HS30 and a sharp increase in response to HS38 (159 % on average). Although this response was less pronounced during grain filling, the general pattern persisted. Notably, 'Primabella' showed significantly lower E relative to the rest of the tested varieties (Fig. 1D).

The differential stomatal response, and therefore E, across developmental stages further translated into similar patterns in ΔT (Fig. 2G and H; $R^2 = 0.94$ for ΔT vs. E, data not shown). No differences were detected in ΔT between varieties at flower spike emergence; however, a more variety-dependent response was evident at grain filling. 'Primadonna' and 'Mandelup' were most efficient at cooling their leaves, while 'Primabella' showed the lowest ΔT (Fig. 2G and H).

3.3. Variety dependent sensitivity of dark reactions under heat stress

To gain deeper insights into the impact of heat stress on the photosynthetic performance, the V_{cmax} and J_{max} parameters were derived from A_n/C_i response curves. These parameters were normalized to 25 °C, allowing an examination of dark reaction levels, without the confounding effect of temperature. Both HS30 and HS38 significantly reduced V_{cmax} relative to CT23 in both developmental stages (Fig. 3A). At flower spike emergence, the V_{cmax} decreased with increasing

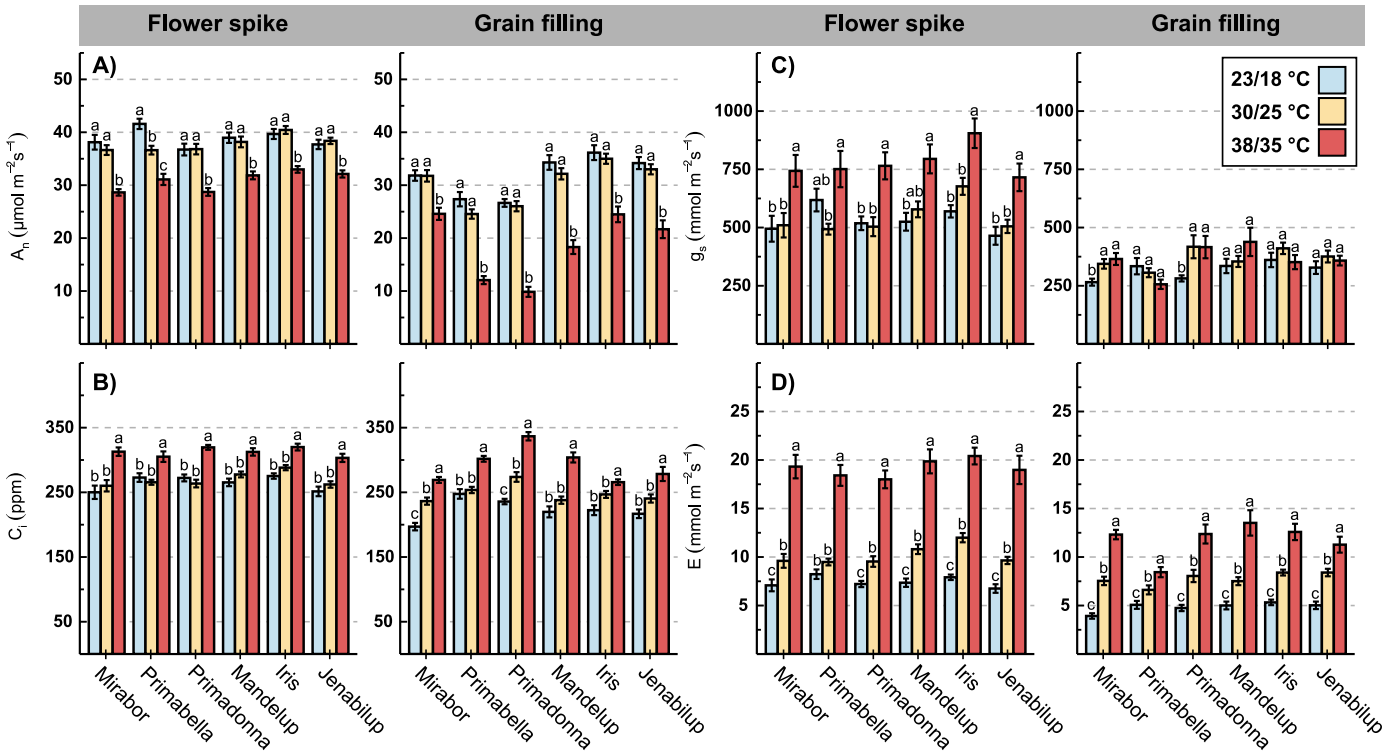

Fig. 1. Leaf gas exchange measurements at 1500 µmol m^{-2} s^{-1} PPFD. **A**) Net photosynthetic assimilation rate (A_n), **B**) Stomatal conductance (g_s), **C**) Intercellular CO_2 (C_i), **D**) Transpiration rate (E). The temperature treatments CT23, HS30, and HS38 are indicated in colour as light blue, yellow, and red, respectively. The data show means ± standard error (SE) (n = 11–16). The compact letter display indicates differences between treatments within variety and stage of development. For differences between varieties within treatments and developmental stages, please refer to supplementary materials. (For interpretation of the references to colour in this figure legend, the reader is referred to the Web version of this article.)

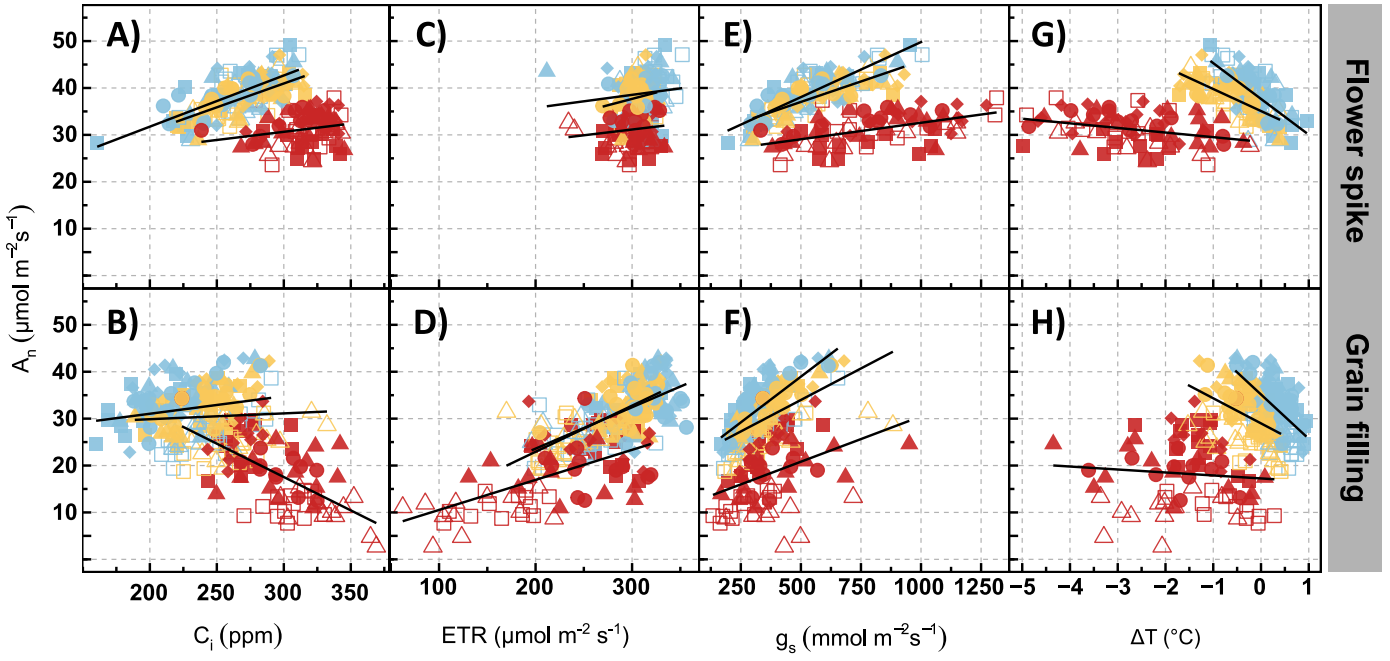

Fig. 2. Relationships between the net CO_2 assimilation rate (A_n) and **A**, **B**) intercellular CO_2 concentration (C_i); **C**, **D**) electron transport rate (ETR); **E**, **F**) stomatal conductance (g_s), and **G**, **H**) leaf cooling (**Δ**T), during flower-spike emergence and grain filling separately. The blue, yellow, and red colours indicate the control, mild heat-stress, and severe heat-stress, respectively. Varieties are represented by following symbols: ■ (Mirabor), □ (Primabella), △ (Primadonna), ▲ (Mandelup), ◆ (Iris), ● (Jenabillup). (For interpretation of the references to colour in this figure legend, the reader is referred to the Web version of this article.)

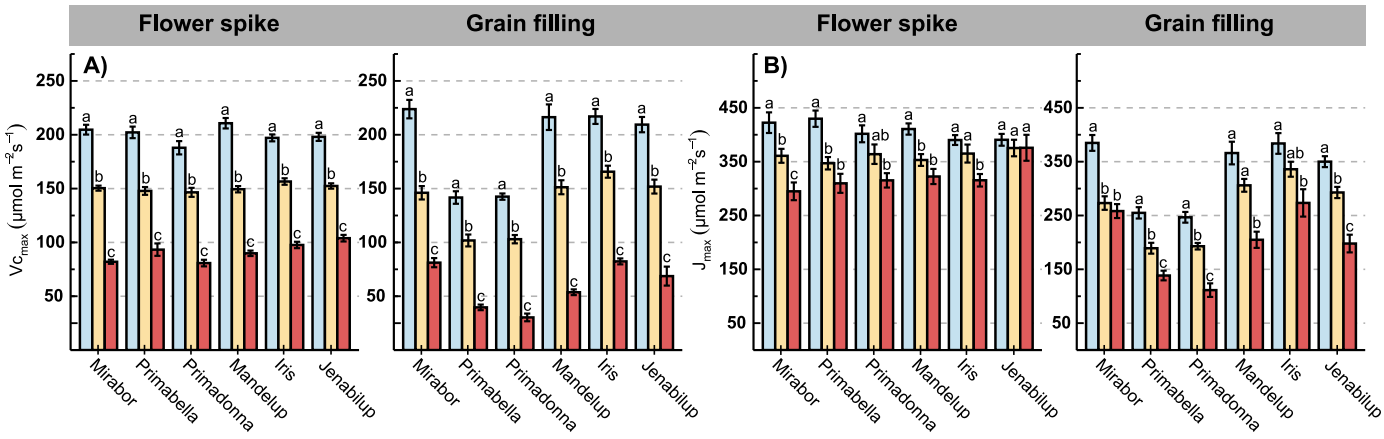

Fig. 3. Parameters derived from A_n/C_i curves normalized to 25 °C; **A**) maximum carboxylation rate of RuBP by Rubisco (V_{cmax}), **B**) maximum RuBP regeneration rate (J_{max}); The temperature treatments CT23, HS30, and HS38 are indicated in colour as blue, yellow, and red, respectively. The data show means ± SE (n = 10–16). The compact letter display indicates differences between treatments within variety and stage of development. For differences between varieties within treatments and developmental stages, please refer to supplementary materials. (For interpretation of the references to colour in this figure legend, the reader is referred to the Web version of this article.)

temperature without a significant genotypic variation (−25 %, −54 % for HS30, HS38, respectively). However, distinct varietal responses in V_{cmax} emerged at grain filling ($p < 0.0001$). Notably, 'Primabella' and 'Primadonna' displayed the lowest V_{cmax} values under CT23 conditions compared to other varieties (≤143 µmol m^{-2} s^{-1}; Table S2). This trend continued under both HS30 and HS38 conditions, where V_{cmax} values for 'Primabella' and 'Primadonna' further declined by 72 % and 79 %, respectively, under HS38. 'Mirabor' and 'Iris' were most capable at maintaining their V_{cmax} potentials (Fig. 3A).

Comparable trends, though with notable exceptions, were observed in the J_{max} response. At flower spike emergence, 'Jenabillup' was the only variety capable of maintaining J_{max} at CT23 levels in both heat treatments (Fig. 3B). Additionally, 'Primadonna' and 'Iris' maintained the control J_{max} level at HS30, with significant reductions at HS38 ($p <$ 0.0001). At grain filling, the control J_{max} of 'Primabella' and 'Primadonna' was significantly lower than the other varieties, with the same pattern persisting across all temperature treatments (Table S2). 'Mirabor' and 'Iris' showed the lowest relative reductions of J_{max} at HS38, amounting to 33 % and 29 % respectively. (Fig. 3B).

3.4. Genotypic variation in photorespiration response to heat stress, modulated by developmental stage

To gain a better understanding about the Rubisco activity under the tested temperature treatments, the P_r was estimated according to Valentini et al. (1995). Strong effects of treatment ($p < 0.0001$) and variety ($p < 0.0001$) were found. The temperature treatments had no effect on P_r in 'Primabella' and 'Primadonna' during flower spike emergence. In contrast, other varieties exhibited a slight reduction in P_r at HS30, and a significant increase at HS38 (15 % on average; Fig. 4). During grain filling, the control P_r in 'Primabella' and 'Primadonna' was significantly lower than the other varieties (Table S2). 'Primadonna' exhibited a

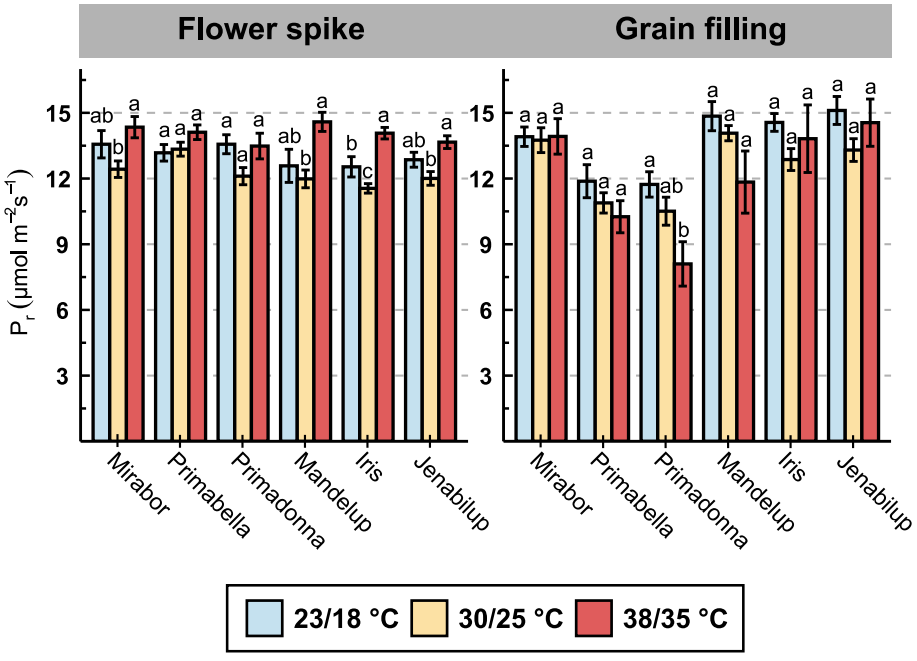

Fig. 4. Rates of photorespiration (P_r), estimated according to Valentini et al., (1995). Lowercase letters indicate differences between treatments within variety. For differences between varieties within treatments please refer to supplementary materials (n = 11–16).

significant reduction in P_r in response to HS38 (−36 %), whereas the remaining varieties maintained P_r at control levels.

3.5. VARIETY-DEPENDENT responses of light reactions under heat stress

To gain further insight into the limitations in the photosynthetic assimilation associated with the light reactions, chlorophyll fluorescence quenching parameters were quantified. The analysis revealed significant impacts of temperature treatments ($p < 0.0001$) on F_v/F_m, with notable varietal distinctions ($p < 0.0001$), particularly during the grain filling stage (Fig. 5A). At flower spike emergence, only 'Primabella' showed a significant reduction in F_v/F_m in response to HS30, while HS38 caused a modest but significant reduction in all varieties. At grain filling, 'Mirabor' was the only variety capable of maintaining F_v/F_m at control levels under HS30. The HS38 caused a significant reduction in F_v/F_m, however, to a differing extent depending on variety (Fig. 5A). 'Mirabor', 'Iris', and 'Jenabillup' were the most capable at maintaining their F_v/F_m (≥0.74), while 'Primabella' and 'Primadonna' showed the lowest values (0.61, 0.51, respectively). The disruption of PETC by the stress treatments, as indicated by F_v/F_m, is also seen in its capacity for electron transport. At flower spike emergence, 'Mandelup', 'Iris', and 'Jenabillup' could maintain their CT23 ETR under both HS30 and HS38, while a modest but significant reduction was observed in the other varieties (Fig. 5). At grain filling, 'Primabella' and 'Primadonna' showed the lowest ETR, together with the highest NPQ (≥0.92) at CT23 relative to the rest of the varieties (Table S3). The HS38 caused a significant ETR reduction in all varieties, but 'Mirabor', 'Iris', and 'Jenabillup' showed the best ability to maintain their PETC (Fig. 5B).

3.6. Varieties better at maintaining photosynthesis under heat stress outperform in yield

The yield performance was examined across three parameters: yield, grain count, and TGW. The effect of heat stress was again very dependent on the stage of development. While the heat stress showed no effect on any of the yield related parameters at flower spike emergence, a variety-dependent response was evident at grain filling (Table 1). Generally, 'Primabella' and 'Primadonna' performed poorly across all treatments relative to the rest of the varieties (Table 1). HS38 caused a significant reduction in TGW for 'Primadonna' and 'Mandelup' (−26 % and −12 %, respectively). It also led to a marked decrease in grain count in 'Primabella' (−30 %) and lowered the yield in 'Primadonna' (−37 %).

In contrast with the plants exposed to heat stress at flower spike emergence (Fig. 6A, B, and 6C), a strong positive relationship between physiological and yield performance parameters was found in plants treated at grain filling (Fig. 6D, E, and 6F). The physiological parameters of 'Primabella' and 'Primadonna' were negatively affected by elevated temperature, while also performing poorly in terms of yield parameters. Under CT23, measured at grain filling, significant positive relationships between yield and regulated energy dissipation parameters [NPQ, q_N, Y (NPQ)], F_q'/F_m' and q_L were found. Under mild and severe heat stress, significant negative relationships between TGW, grain count, and yield with Y(NPQ) and Y(NO) remained. Additionally, strong positive relationships were found between these yield parameters and parameters of dark reactions of photosynthesis (V_{cmax}, J_{max}, A_n, P_r), and parameters of absorbed energy transfer and utilization (ETR, F_v/F_m, q_L).

3.7. Contrasting shift in grain nutritional composition under heat stress in sensitive and tolerant varieties

To gain a deeper understanding of yield performance, a proximal nutritional analysis was performed on grains of four varieties with contrasting physiological responses to heat stress: 'Mirabor', 'Primabella', 'Primadonna', and 'Iris' (Table 2). HS38 significantly affected grain protein ($p < 0.01$), lipid ($p < 0.0001$), carbohydrate ($p < 0.01$), ash ($p < 0.01$), and moisture content ($p < 0.001$). 'Primabella' and 'Primadonna', which underperformed across several physiological and yield parameters, exhibited a notable increase in grain protein content (17 % and 21 %, respectively) alongside a reduction in carbohydrates (−7 % and −16 %, respectively). In contrast, no significant changes in these components were observed in 'Mirabor', while 'Iris' showed a marked decrease in carbohydrate content (−13 %) with a concurrent increase in grain lipid content under HS38 (41 %). Lastly, both 'Mirabor' and 'Primadonna' had a rise in grain ash content in response to heat stress.

To further investigate the effects of heat stress on yields of specific grain nutritional components, we have calculated protein and carbohydrate yields (Y_{Prot}, Y_{Carb}, respectively). We have found no effect of heat stress on the Y_{Prot} in any of the tested varieties, while a significant reduction in Y_{Carb} was detected in 'Primabella' and 'Primadonna' (Table S4).

A strong relationship between grain nutritional components and physiological parameters under the severe heat stress at grain filling was

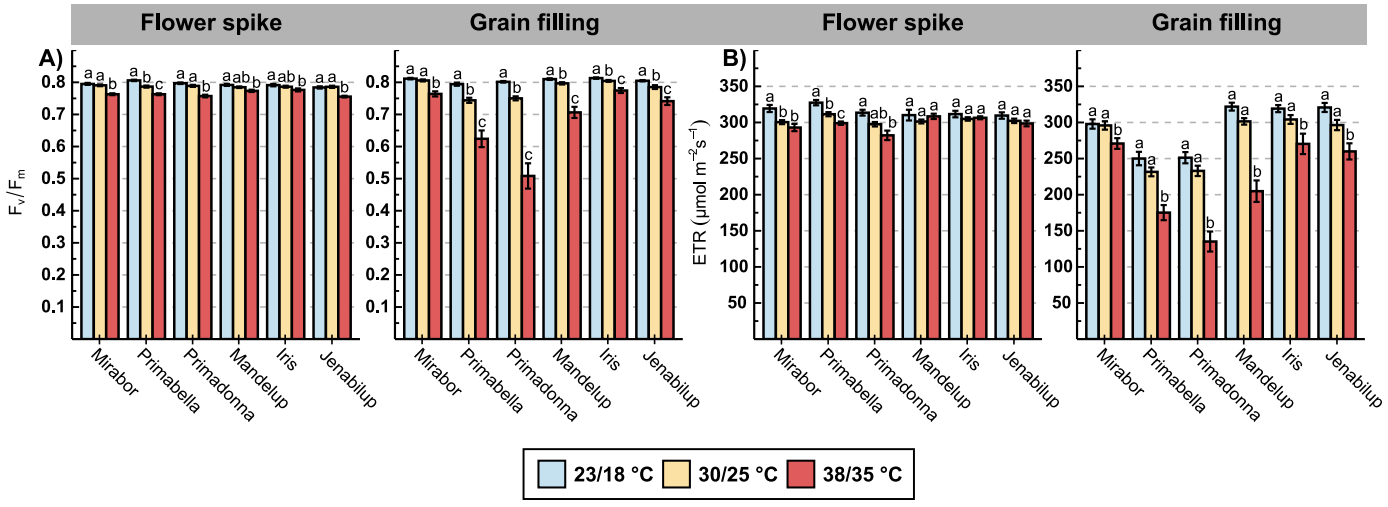

Fig. 5. Chlorophyll fluorescence quenching parameters measured at 1500 µmol m^{-2} s^{-1} PPFD; **A**) Maximum quantum efficiency of PSII (F_v/F_m) on dark-adapted leaves, and **B**) Electron transport rate (ETR). The temperature treatments CT23, HS30, and HS38 are indicated in colour as blue, yellow, and red, respectively. The data show are means ± SE (n = 10–16). The compact letter display indicates differences between treatments within variety and stage of development. For differences between varieties within treatments please refer to supplementary materials. (For interpretation of the references to colour in this figure legend, the reader is referred to the Web version of this article.)

Table 1
Yield related parameters: thousand grain weight (TGW), grain count, and yield, shown as means ± SE. The three temperature treatments indicated as C23 (control), HS30 (mild heat stress), and HS38 (severe heat stress). Uppercase letters indicate significant differences between varieties within treatments; lowercase letters indicate differences between treatments within varieties.

Variety	Treatment	Flower-spike emergence			Grain Filling		
		TGW (g)	Grains (n plant^{-1})	Yield (g plant^{-1})	TGW (g)	Grains (n plant^{-1})	Yield (g plant^{-1})
Mirabor	CT23	106.65 ± 2.48 $^{A\ a}$	217.81 ± 41.08 $^{A\ a}$	23.22 ± 1.08 $^{A\ a}$	107.44 ± 2.18 $^{AB\ a}$	192.81 ± 53.2 $^{A\ a}$	20.86 ± 1.25 $^{A\ a}$
	HS30	105.75 ± 5.85 $^{A\ a}$	245.67 ± 22.55 $^{A\ a}$	26.15 ± 1.47 $^{A\ a}$	106.59 ± 2.24 $^{A\ a}$	233.31 ± 51.68 $^{A\ a}$	24.99 ± 1.21 $^{A\ a}$
	HS38	100.28 ± 7.74 $^{A\ a}$	174.31 ± 18.68 $^{A\ a}$	17.62 ± 1.51 $^{A\ a}$	116.05 ± 4.58 $^{A\ a}$	235.63 ± 27.32 $^{A\ a}$	27.36 ± 1.36 $^{A\ a}$
Primabella	CT23	57.01 ± 4.49 $^{C\ a}$	126.13 ± 23.37 $^{B\ a}$	7.48 ± 0.83 $^{C\ a}$	66.58 ± 3.51 $^{C\ a}$	234.63 ± 13.49 $^{A\ a}$	15.61 ± 0.63 $^{A\ a}$
	HS30	65.45 ± 8.53 $^{B\ a}$	141.81 ± 28.99 $^{A\ a}$	10.32 ± 1.29 $^{A\ a}$	65.79 ± 1.93 $^{C\ a}$	185.94 ± 30.78 $^{A\ ab}$	12.29 ± 0.6B $^{C\ a}$
	HS38	69.41 ± 3.15 $^{B\ a}$	171.63 ± 36.5 $^{A\ a}$	12.11 ± 0.86 $^{A\ a}$	70.43 ± 2.69B $^{C\ a}$	168.85 ± 13.62 $^{A\ b}$	11.95 ± 0.6B $^{C\ a}$
Primadonna	CT23	74.29 ± 6.76 $^{B\ a}$	143.31 ± 10.96 $^{AB\ a}$	10.64 ± 0.86 $^{BC\ a}$	92.03 ± 3.57 $^{B\ a}$	158.56 ± 15.25 $^{A\ a}$	14.65 ± 0.79 $^{A\ a}$
	HS30	87.35 ± 2.99 $^{AB\ a}$	138.19 ± 11.8 $^{A\ a}$	12.14 ± 0.69 $^{A\ a}$	80.35 ± 2.35 $^{B\ b}$	148.17 ± 11.97 $^{A\ a}$	11.92 ± 0.53 $^{C\ ab}$
	HS38	84.96 ± 5.42 $^{AB\ a}$	151.19 ± 20.0 $^{A\ a}$	13.21 ± 1.27 $^{A\ a}$	67.23 ± 2.57 $^{C\ c}$	138.38 ± 19.37 $^{A\ a}$	9.32 ± 0.49 $^{C\ b}$
Mandelup	CT23	97.38 ± 3.32 $^{A\ a}$	126.75 ± 13.54 $^{B\ a}$	12.41 ± 0.79 $^{ABC\ a}$	105.48 ± 6.46 $^{AB\ ab}$	182.88 ± 15.14 $^{A\ a}$	19.58 ± 1.48 $^{A\ a}$
	HS30	93.81 ± 9.78 $^{AB\ a}$	180.94 ± 19.58 $^{A\ a}$	16.11 ± 0.49 $^{A\ a}$	110.17 ± 2.38 $^{A\ a}$	219.75 ± 11.16 $^{A\ a}$	24.24 ± 0.76 $^{A\ a}$
	HS38	99.27 ± 11.3 $^{A\ a}$	161.81 ± 11.73 $^{A\ a}$	15.56 ± 0.77 $^{A\ a}$	89.7 ± 7.16 $^{AB\ b}$	242.06 ± 21.59 $^{A\ a}$	22.28 ± 1.70 $^{AB\ a}$
Iris	CT23	101.46 ± 2.16 $^{A\ a}$	175.56 ± 13.71 $^{AB\ a}$	17.77 ± 0.47 $^{AB\ a}$	106.07 ± 3.5 $^{AB\ a}$	226.94 ± 31.36 $^{A\ a}$	23.82 ± 0.94 $^{A\ a}$
	HS30	92.41 ± 10.16 $^{AB\ a}$	146.13 ± 21.47 $^{A\ a}$	14.4 ± 1.67 $^{A\ a}$	107.63 ± 1.76 $^{A\ a}$	233.06 ± 24.24 $^{A\ a}$	25.1 ± 0.74 $^{A\ a}$
	HS38	106.39 ± 4.67 $^{A\ a}$	188.88 ± 22.34 $^{A\ a}$	20.29 ± 1.29 $^{A\ a}$	95.83 ± 14.42 $^{A\ a}$	240.02 ± 23.23 $^{A\ a}$	22.9 ± 2.28 $^{AB\ a}$
Jenabillup	CT23	105.53 ± 3.25 $^{A\ a}$	157.06 ± 11.65 $^{AB\ a}$	16.62 ± 0.81 $^{AB\ a}$	117.35 ± 6.36 $^{A\ a}$	216.06 ± 7.83$^{A\ a}$	25.34 ± 1.27$^{A\ a}$
	HS30	107.66 ± 8.6 $^{A\ a}$	165.56 ± 8.19 $^{A\ a}$	18.11 ± 1.96 $^{A\ a}$	109.04 ± 3.55 $^{A\ a}$	188.08 ± 37.56$^{A\ a}$	20.26 ± 1.09$^{AB\ a}$
	HS38	99.04 ± 11.35 $^{A\ a}$	180.25 ± 16.35 $^{A\ a}$	18.65 ± 2.31 $^{A\ a}$	106.98 ± 7.98 $^{A\ a}$	239.94 ± 29.56$^{A\ a}$	26.63 ± 2.35$^{A\ a}$

found. For example, the grain protein contents showed a significant negative correlation with V_{cmax} and ETR, as well as a strong positive correlation with NPQ. However, grain lipid contents showed significant positive correlation with A_n, V_{cmax}, and J_{max} (data not shown).

3.8. PCA reveals distinct phenotypic responses to heat stress at different developmental stages

Furthermore, a PCA was performed to more holistically evaluate the driving factors of treatment- and variety-dependent responses of plants at the two developmental stages. In plants treated at flower spike emergence, the PC1 and PC2 explained 47.06 % and 13.78 % of the variability, respectively (Fig. 7A) and we primarily observed a separation along the PC1. This separation was driven by changes in plant water relations (g_s, E, ΔT) and carbon balance parameters (R_d, LCP, C_i) under severe heat stress, while control plants showed higher photoprotective and photosynthetic parameters, including regulated energy dissipation [Y(NPQ), NPQ, q_N], photosynthetic performance (e.g., F_v/F_m, A_n, A_{max}, V_{cmax}, ETR, θ, α), and water-use efficiency (WUE_i, WUE_{leaf}). While PC2 captured variation in yield-related traits and certain fluorescence parameters, it did not result in distinct clustering.

In plants treated at grain filling, the PC1 and PC2 explained 48 % and 19.66 % of the variability, respectively (Fig. 7B). Similarly to flower spike emergence, we observed a treatment-dependent separation along the PC1, driven by plant water relations (E, ΔT), carbon balance parameters (C_i, LCP), and nutritional components (ash, protein) under the severe heat stress; while the control differs in water-use efficiency parameters (WUE_i, WUE_{leaf}), and photosynthetic performance including the parameters of light (F_v/F_m, F_q'/F_m', θ, ETR) and dark (V_{cmax}, J_{max}, A_{max}, A_n) reactions of photosynthesis, yield and nutritional composition related parameters (carbohydrates and moisture). In contrast to the response at flower spike emergence, a clear variety-dependent separation along PC2 was seen at grain filling (Fig. 7B) under both control and heat stress conditions. The separation of heat-tolerant and sensitive clusters was driven by differences in regulated energy dissipation [Y(NPQ), NPQ, q_N], plant water relations (g_s, E, ΔT), carbon balance (R_d, LCP) and nutritional parameters (such as grain lipid content).

4. Discussion

This study provides novel insights into the physiological and agronomic responses of *L. angustifolius* to short-term heat stress imposed at two critical reproductive stages. By integrating gas exchange, chlorophyll fluorescence, yield traits, and grain nutritional composition, we demonstrated that both the developmental stage at which heat occurred and varietal differences significantly influenced the degree of stress sensitivity. Notably, photosynthetic traits such as net CO_2 assimilation and PSII efficiency were strongly correlated with yield performance and grain quality under heat stress, emphasizing their potential as robust selection criteria in breeding programs. While physiological phenotyping is widely used to identify stress-tolerant genotypes, such approaches rarely account for the effects of stress on grain nutritional quality—despite its critical role in determining the overall value and adoption potential of novel legume crops. Our findings address this gap and underscore the importance of integrating physiological and grain nutritional traits when evaluating varietal performance under climate stress.

4.1. Heat induced Rubisco limitation suppresses net photosynthesis at flower spike emergence

Temperatures above the physiological optimum are known to reduce the A_n (Mathur et al., 2014; Ahmad et al., 2025). In this experiment a heat stress at flower spike emergence caused a reduction in A_n, with a concurrent accumulation of the intercellular CO_2 in all tested lupin varieties (Figs. 1 and 2). This aligns with results from Akula et al. (2024), Abdelhakim et al. (2022a), Chovancek et al. (2019) on wheat, as well as Carmo-Silva and Salvucci (2012) on legumes. This indicates reduced rates of RuBP carboxylation by the Rubisco enzyme, as evidenced by the reduction in the standardized V_{cmax} (Fig. 3). Similar response was documented by Sommer et al. (2024), experimenting on wheat. On the other hand, the P_r at HS38 was significantly higher relative to HS30 in the heat tolerant varieties, while the susceptible 'Primabella' and 'Primadonna' showed control levels (Fig. 4). We concluded that this is caused by reduction of CO_2 solubility, and increased Rubisco specificity towards O_2 at high temperatures (Jordan and Ogren, 1984; Dusenge et al., 2019).

4.2. Electron transport chain stability during heat stress is supported by photorespiration

Photorespiration supports electron transport in the thylakoid

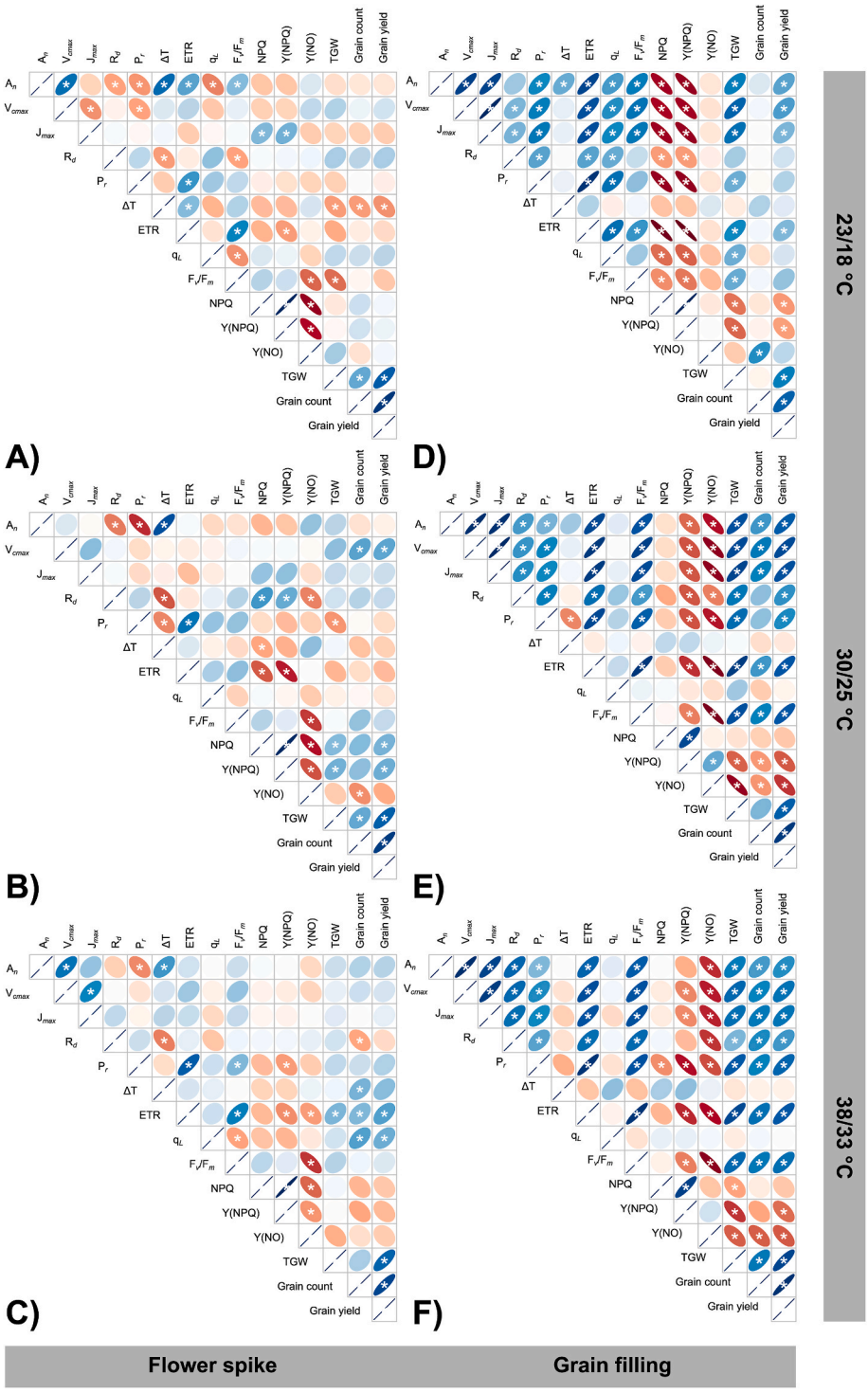

Fig. 6. Pearson correlations between selected physiological and yield component parameters under CT23, HS30 and HS38 conditions, during flower spike emergence (**A**, **B**, **C**) and grain filling (**D**, **E**, **F**) separately. Blue and red hues indicate positive and negative correlations, respectively, with asterisks indicating the p-value of a given relationship below $\alpha < 0.05$. (For interpretation of the references to colour in this figure legend, the reader is referred to the Web version of this article.)

membrane by consuming excess reducing power and energy (NADPH, ATP), thereby preventing accumulation and allowing the light-dependent reactions to proceed efficiently (Bauwe, 2023; de Souza et al., 2024; Eisenhut et al., 2019; Voss et al., 2013). This contributes to the prevention of the PETC over-reduction, and thus photoinhibition as evidenced by biologically insignificant reductions in F_v/F_m in all varieties. This agrees with our results, where ETR was maintained at control levels in 'Mandelup', 'Iris', and 'Jenabillup', while a modest reduction was observed in the other varieties (Fig. 5).

Beyond its photoprotective role, photorespiration functions as a crucial redox valve under stress, helping to dissipate excess electrons and avoid ROS build-up—particularly under conditions where CO_2 fixation is impaired, such as heat or drought stress (Voss et al., 2013; Wingler et al., 2000). The process not only consumes ATP and NADPH but also helps stabilize chloroplast redox balance and interacts dynamically with mitochondrial and peroxisomal metabolism (Eisenhut et al.,

Table 2
Proximal nutritional analysis of Lupin grains exposed to control temperatures and severe heat stress at grain filling expressed in g per 100 g of grain powder. The uppercase letters indicate differences between varieties within treatments, while */ns indicates the effect of treatment within variety.

Variety	Treatment	Protein	Carbohydrates	Lipids	Ash	Moisture
Mirabor	CT23	25.3 ± 0.4 $^{A\ ns}$	59.4 ± 0.4 $^{A\ ns}$	7.6 ± 0.3 $^{A\ ns}$	4.4 ± 0.05 ^{A*}	3.2 ± 0.5 ^{A*}
	HS38	28.7 ± 1.5 ^{B}	57.0 ± 1.6 ^{A}	7.3 ± 0.5 ^{B}	5.1 ± 0.04 ^{A}	1.8 ± 0.3 ^{A}
Primabella	CT23	25.3 ± 0.5 ^{A*}	61.4 ± 0.3 ^{A*}	6.8 ± 0.3 $^{AB\ ns}$	4.8 ± 0.1 $^{A\ ns}$	1.8 ± 0.2 $^{B\ ns}$
	HS38	30.6 ± 0.8 ^{AB}	57.3 ± 1.0 ^{A}	6.5 ± 0.1 ^{B}	5.2 ± 0.1 ^{A}	0.5 ± 0.3 ^{B}
Primadonna	CT23	28.0 ± 1.0 $^{A\ *}$	59.3 ± 0.8 ^{A*}	5.8 ± 0.2 $^{B\ ns}$	5.0 ± 0.1 ^{A*}	1.9 ± 0.1 $^{B\ *}$
	HS38	35.4 ± 0.4 ^{A}	50.8 ± 0.5 ^{B}	6.9 ± 0.6 ^{B}	5.7 ± 0.1 ^{A}	1.3 ± 0.3 ^{AB}
Iris	CT23	27.7 ± 1.2 $^{A\ ns}$	60.8 ± 1.5 ^{A*}	5.8 ± 0.3 $^{B\ *}$	4.6 ± 0.1 $^{A\ ns}$	1.1 ± 0.1 $^{B\ ns}$
	HS38	30.3 ± 1.8 ^{AB}	53.7 ± 1.6 ^{AB}	9.9 ± 0.7 ^{A}	5.2 ± 0.2 ^{A}	0.9 ± 0.5 ^{AB}

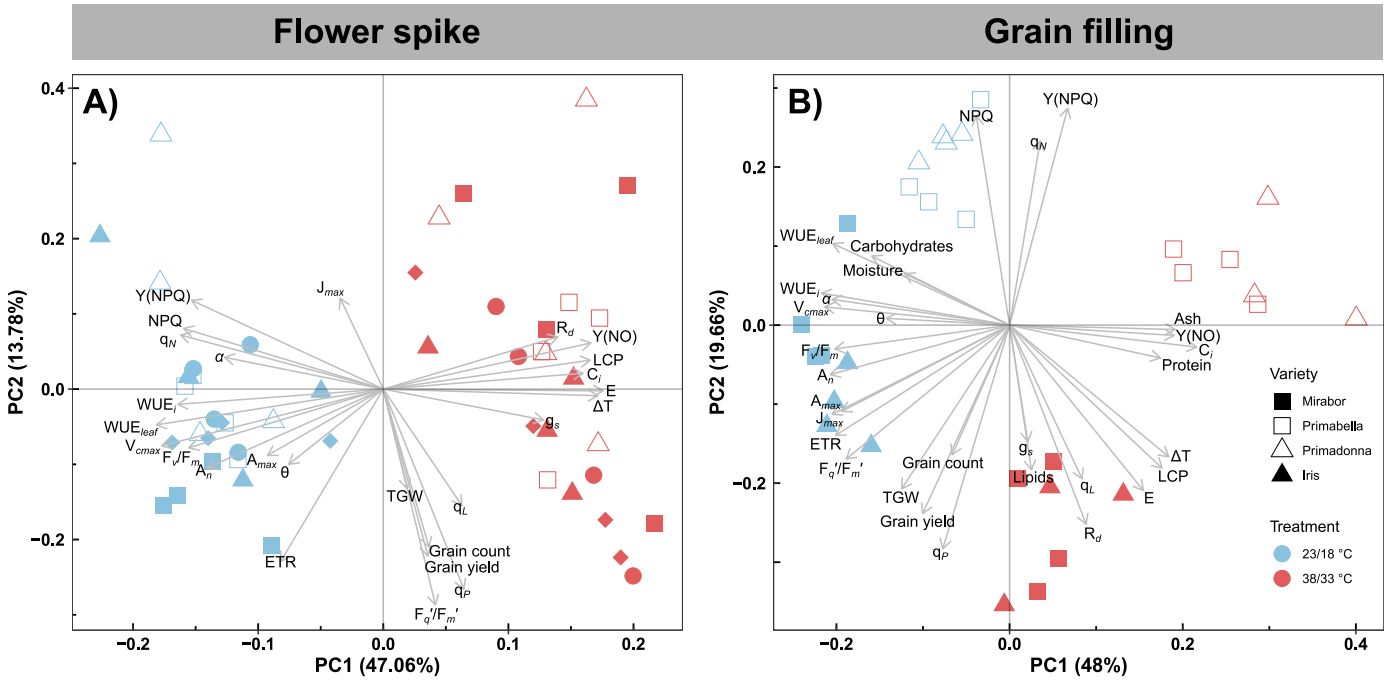

Fig. 7. Principial component analysis of gas exchange, chlorophyll fluorescence, yield components, and grain nutritional composition parameters, in response to control and severe heat stress; separately for: **A)** plants treated at flower spike emergence, and **B)** grain filling.

2019). Additionally, the production of H_{2O2} during glycolate oxidation in peroxisomes may serve as a signalling intermediate in redox-regulated stress responses (Voss et al., 2013). This buffering capacity may explain the maintenance of RuBP regeneration rates under heat stress, with a notable case in 'Jenabillup', where J_{max} remained stable (Fig. 3).

Thus, while the dark reactions appear more vulnerable to heat stress—as shown in the decline of V_{cmax} and J_{max} in most varieties (Crafts-Brandner and Law, 2000; Scafaro et al., 2023)—photorespiration helps protect the photosynthetic apparatus by alleviating redox imbalances. This aligns with recent perspectives that frame photorespiration not as wasteful, but as an integral, dynamic component of stress resilience and photosynthetic optimization under fluctuating environments (Bauwe, 2023; Timm and Hagemann, 2020).

4.3. *Leaf cooling protects the photosynthetic apparatus at flower spike emergence despite biochemical constraints induced by heat stress*

Plants often increase stomatal conductance in response to heat stress as a cooling mechanism, a pattern observed in previous studies (Deva et al., 2020; Chen et al., 2025; Diao et al., 2024; Urban et al., 2017; Devi et al., 2023). In our experiment, the stomatal conductance and transpiration remained high under the HS38 relative to control in all varieties as seen in Fig. 1 (Urban et al., 2017; Sharma et al., 2015; Chen et al., 2025). Thus, it can be asserted that, despite the reduced V_{cmax} and higher R_d, the intercellular CO_2 did not reach sufficiently high levels to induce reduction in g_s (Engineer et al., 2016). This resulted in significant ΔT (Fig. 2), further mitigating the effects of heat stress by maintaining the photosynthetic apparatus closer to its thermal optimum (Deva et al., 2020; Poudyal et al., 2018; Sharma et al., 2015).

4.4. *Grain filling heat stress triggers contrasting photosynthetic losses across varieties, buffered by photorespiration*

Interestingly, at grain filling the heat stress elicited a markedly different physiological response compared to flower spike emergence, with significant varietal differences. Both mild and severe heat stress induced an overall reduction in Rubisco activity, attributed to high rates of inactivation of Rca (Carmo-Silva and Salvucci, 2012; Khanzada et al., 2025). 'Primabella' and 'Primadonna' showed the highest reduction in Rubisco activity, with a concurrent highest C_i (Figs. 1 and 4). Thus, the insufficient cycling of substrates for the light dependent reactions likely led to a gradual over-reduction of PETC and photoinhibition, as seen by the significant reductions in ETR and F_v/F_m (Fig. 5). On the other hand, 'Mirabor', 'Iris', and 'Jenabillup' maintained higher levels in photosynthetic parameters of light (ETR, F_v/F_m) and dark reactions (A_n, P_r, V_{cmax}). Interestingly, similar findings were reported by Akula et al. (2024), who observed significant effects of developmental stage, with

more pronounced varietal differences at later stages (anthesis) compared to earlier stages (stem elongation), as evidenced by distinct cluster separation in the PCA analysis. In all varieties, the percentage reduction in metabolic activity under HS38 relative to CT23 followed the pattern: A_n (23–62 %) > ETR (9–45 %) > P_r (0–34 %). This suggests that P_r plays a crucial role in maintaining electron transport when A_n is significantly inhibited.

4.5. Heat stress-induced stomatal adjustments at grain filling reflect Rubisco decline and cooling efforts, with a shift in water allocation toward developing grains

Our results showed a clear divergence in stomatal conductance responses to heat stress across developmental stages, with a marked lack of stomatal response at grain filling compared to flower spike emergence (Fig. 1). A modest yet statistically significant increase in g_s under heat was observed only in 'Mirabor' and 'Primadonna', while the remaining varieties maintained g_s at control levels. This response may be linked to a general decline in Rubisco activity under heat, accompanied by a rise in intercellular CO_2 concentration (C_i), which signals downregulation of g_s to align CO_2 supply with reduced assimilation capacity (Carmo-Silva and Salvucci, 2012). This was reflected in lower transpiration and ΔT across all varieties, potentially exacerbating thermal stress (Fig. 2).

These findings align with previous research suggesting that stomatal behaviour may shift depending on developmental stage and carbon economy (Akula et al., 2024). During flower spike emergence, plants appeared to prioritize carbon gain over water conservation, maintaining photosynthesis to support developing reproductive tissues and the accumulation of carbon reserves needed for grain filling. At this stage, mechanisms like transpirational leaf cooling are clearly favoured to protect photosynthetic function and avoid premature leaf loss. In contrast, during grain filling, the role of leaves shifts to serving primarily as sources for assimilate translocation. Here, the plant exhibits reduced stomatal conductance under heat stress, reflecting a strategy to conserve water. Excess water loss at this stage could increase phloem sap viscosity, elevate hydraulic resistance and impair assimilate flow toward developing grains—ultimately compromising reproductive success (Woodruff, 2014; Stanfield and Bartlett, 2022). Thus, stomatal regulation may prioritize maintaining phloem function over photosynthetic performance. This interpretation supports and potentially extends the framework proposed by (Blonder et al., 2023), who posits that leaves are shed when the water cost of thermal protection outweighs the carbon benefit of retention. Our findings suggest that not only the possibility, but perhaps the necessity of future carbon gain determines stomatal behaviour—critical at early reproductive stages but deprioritized at grain filling when efficient carbon translocation becomes paramount at the expense of leaf tissue temperature (Sarto et al., 2017). By demonstrating that developmental stage plays a critical role in determining whether stomata prioritize heat avoidance or resource allocation, our work addresses an important gap in the understanding of stomatal behaviour in hot environments.

4.6. VARIETY-DEPENDENT yield responses to grain filling heat stress align with photosynthetic decline

Heat stress at reproductive development can reduce the grain legume yields through a variety of interconnected mechanisms. These are associated with photosynthetic assimilation, assimilate translocation and partitioning, which affects reproductive organ development, as well as the activity of enzymes involved in carbohydrate and protein biosynthesis in grains (Boyer and McLaughlin, 2007; Sita et al., 2017, 2018; Sumesh et al., 2008). Yield losses of legumes exposed to heat stress during anthesis depend on the species and intensity of the stress. These can range from 10 % in chickpea at 26 °C, to 90 % yield reduction in peanut at 44 °C day temperatures (Farooq et al., 2017). In an experiment conducted by Jansen et al. (2009), lupins grown at 20 °C until anthesis were exposed to 30 °C for one month, which resulted in a failure to set pods. Additionally, three lupin varieties were exposed to temperatures of 30/16 °C from flowering until pod ripening in a chamber experiment. This resulted in extreme reductions in pods per plant, grains per plant, and overall yield. The minimum reductions observed were 56 %, 81 %, and 92 %, in respective parameter, in 'Probor'. In our experiment, the plants exposed to heat stress at flower spike emergence begun flowering during the five days of temperature treatment. However, in contrast with majority of the literature we did not find a significant effect of heat stress on any of the measured yield parameters (Table 1).

Leaf photosynthesis rate and leaf carbohydrate contents are closely related (Proietti et al., 2023; Zhou et al., 2017). A reduction in leaf photosynthesis can lead to a gradual depletion of leaf carbohydrate reserves and reduced sucrose translocation towards the reproductive organs (Boyer and McLaughlin, 2007; Sita et al., 2017). Furthermore, a reduction of glucose and starch contents in developing reproductive organs has been linked to decreasing photosynthetic assimilation under abiotic stress (Boyer and McLaughlin, 2007). Plants can cope with short-term disruptions of photoassimilation through utilization of carbon reserves from roots and stems. These reserves can become critical especially during the short-term heat stress, when the photosynthetic assimilation are limited, and R_d increases significantly (Boyer and McLaughlin, 2007; Sita et al., 2017; Farooq et al., 2017; Taria et al., 2025). In line with this, the absence of a measurable yield impact during heat stress at flower spike emergence in our study may suggest that *L. angustifolius* is capable of buffering short-term stress through effective use of internal carbon reserves. Heat stress at anthesis primarily limits the yield by disrupting pod and seed set, which could partly explain the absence of the temperature effect on TGW in this experiment. However, this does not explain the absence of temperature effect on grain count (Table 1). Physiological data measured at flower spike emergence indicate a limited effect of heat stress on light-dependent processes of photosynthesis, and a modest effect on A_n, allowed by maintaining Rubisco activity through P_r and ΔT. Thus, it is possible that the five days of heat stress were not sufficient to trigger a shortage of photo-assimilates for translocation towards reproductive organs, with the possibility of further mitigation through utilization of carbohydrate reserves from roots and stem (Boyer and McLaughlin, 2007; Chaves et al., 2002). Heat stress at grain filling reduces yields through disruption of transport of carbohydrates and biochemical processes involved in synthesis of starch, protein, and lipids (Sita et al., 2017). Additionally, heat stress can disrupt the source-sink relationship by reducing the source strength by inhibiting photoassimilation and directing more photoassimilates towards acclimatory metabolic adjustment (Plaut et al., 2004; Sehgal et al., 2018). These are possible explanations for the observed reduction in grain count, TGW, and yield in the heat sensitive 'Primabella', and 'Primadonna', as these varieties also experienced significant disruption of light- and dark-dependent processes of photosynthesis, leading to possible source limitations as a result of reduced carbon reserves (Figs. 1 and 2).

4.7. Heat stress at grain filling modulates carbohydrate and protein accumulation differently across varieties

The effect of heat stress on yield can be further elucidated by examining its effect on the grain nutritional components. Since starch constitutes a significant portion of seed weight, disruption in its accumulation is the primary factor contributing to yield loss under heat stress (Sita et al., 2017; Yang et al., 2004; Sumesh et al., 2008). The vast majority of studies on heat stress report significant reductions in grain carbohydrate contents (Sarkar et al., 2021; Farooq et al., 2018; Ben Mariem et al., 2021). Carbohydrate accumulation can be inhibited through reduced photosynthate supply, translocation, as well as denaturation of enzymes involved in their synthesis, such as soluble and granule bound starch synthase (Sumesh et al., 2008; Zhou et al., 2017). Our results partially support this, as we see reduced carbohydrate

contents under heat stress in varieties 'Primabella' and 'Primadonna', which also showed marked reductions across a range of photosynthetic parameters, including A_n, thus the photoasimilate supply could have become limiting (Figs. 1 and 3). An interesting exception is 'Iris', where a slight reduction in carbohydrate content, with a concurrent increase in lipids content was observed (Table 2).

The effects of heat stress on grain protein content appear highly dependent on species and stress intensity, as an increase, decrease, and no effect of heat stress has been reported (Rotundo and Westgate, 2009; Farooq et al., 2018; Sarkar et al., 2021). In this experiment, the protein yields per plant did not change in response to heat stress (Table S4), while protein contents per grain increased significantly in the two heat sensitive varieties (Table 2). This could indicate a higher thermal tolerance of grain protein synthesis pathway relative to that of carbohydrates. This was seen in maize under heat stress during grain filling, where grain weight and starch deposition was suppressed due to decreases in enzyme activities involved in starch synthesis, while the protein content increased due to increased activity of glutamate synthase (Yang et al., 2018). Alternatively, the protein biosynthesis could be prioritized at the expense of carbohydrates under heat stress, leading to hydrolyzation of grain starch, with products directed towards increased requirement for mitochondrial respiration, and a proportional increase in grain protein content as a result. Overall, the increase in grain protein concentration did not translate into higher total protein yield per plant, underscoring a key trade-off between grain composition and overall nutritional output under stress.

4.8. Future perspectives

This study highlights the importance of considering both the developmental stage and variety in breeding programs aimed at improving heat tolerance in *L. angustifolius*. The findings suggest that varietal differences in photosynthetic responses and yield losses under heat stress could be leveraged for climate-smart breeding strategies (Ahmad et al., 2023; Pixley et al., 2023; Raza et al., 2024). Future research should focus on the identification of genetic markers associated with heat tolerance, which could facilitate the development of heat-resistant varieties through marker-assisted selection. As outlined by Raza et al. (2024), utilizing physiological mechanisms for QTL identification and gene discovery has been crucial for improvement of crops such as sorghum, wheat, barley, and groundnut (Borrell et al., 2014; Williams et al., 2022; Vadez and Ratnakumar, 2016; Vadez et al., 2012). Additionally, integrating genomic and phenotypic data could further enhance the understanding of heat stress resilience mechanisms, guiding breeding programs toward more targeted approaches (Sharma et al., 2017). Agronomic practices can be refined to mitigate the heat stress, such as optimizing irrigation schedules for improved leaf cooling (Luan and Vico, 2021; Siebert et al., 2017). Moreover, investigating the role of metabolites in heat tolerance could open new avenues for improving the nutritional quality of heat-stressed crops. This is especially true for lupins, that show a significant increase in toxic grain quinolizidine alkaloids content in response to abiotic stress (Jansen et al., 2009; Frick et al., 2018). Long-term integrative *omics* studies exploring the temporal effects of combined heat stress and other abiotic stresses, such as drought, could provide a more comprehensive understanding of how *L. angustifolius* adapts to changing climate conditions as well as the relevance of stress priming in multiple concurrent stress episodes in this crop (Liu et al., 2022; Tugizimana et al., 2018; Provera et al., 2024).

5. Conclusion

In conclusion, the heat stress response of lupin varieties varied significantly across developmental stages. At flower spike emergence, the maintenance of ETR and Rubisco activity through increased P_r and ΔT helped mitigate the effects of elevated temperatures on photosynthesis and yield. The absence of measurable yield reduction during this stage suggests that *L. angustifolius* may buffer short-term heat stress through physiological adjustments and possible mobilization of internal carbon reserves. However, at grain filling, varietal differences became more pronounced. 'Mirabor', 'Iris', and 'Jenabillup' exhibited superior heat tolerance, maintaining both light-dependent (F_v/F_m, ETR) and dark reactions (V_{cmax}, J_{max}), whereas 'Primabella' and 'Primadonna' showed markedly reduced photosynthetic capacity under severe heat stress. These differences extended to yield and grain composition. The observed differences in photosynthetic parameters were mirrored in the yield performance. Varieties that maintained photosynthetic function during grain filling, such as 'Mirabor', 'Iris', and 'Jenabillup', also preserved yield-related traits, including yield, grain count and TGW, whereas 'Primabella' and 'Primadonna' exhibited significant declines. These patterns extended to grain nutritional composition. 'Primabella' and 'Primadonna', which showed the greatest reductions in gas exchange (A_n, V_{cmax}, J_{max}, P_r, R_d) and chlorophyll fluorescence (F_v/F_m), also display a marked decrease in grain carbohydrate content, coupled with an increase in protein levels. In contrast, the more heat-tolerant 'Mirabor' and 'Jenabillup', showed no significant changes in grain composition. These findings underscore the critical role of interdisciplinary phenotyping in breeding for heat tolerance, particularly during grain filling, where differences in photosynthetic function are associated with variations in yield and grain quality. By identifying key physiological traits linked to heat tolerance, this work provides a foundation for future physiological, metabolomic, and molecular studies supporting the development of resilient lupins.

Beyond breeding, the adoption of heat-tolerant *L. angustifolius* varieties offers potential agronomic and economic benefits for European cropping systems. As a legume capable of biological nitrogen fixation, lupin can reduce fertilizer use and support crop diversification, contributing to soil health and sustainability. Its high protein content also aligns with Europe's goal of reducing dependence on imported soy and strengthening plant-based protein self-sufficiency. Economically, heat-resilient varieties may help stabilize yields and reduce risk under increasing heat stress, while preserving grain quality for food and feed markets. Together, these traits suggest that lupin could become a more cost-effective and climate-resilient protein crop, with potential for broader integration into sustainable European agriculture, particularly if heat-tolerant, high-performing varieties are made available and promoted through targeted breeding and policy support.

Author contributions

MK designed and performed the experiment. TM and CP assisted with conducting the experiment and harvesting. OB performed the proximal nutritional analysis and wrote the materials and methods subsection for this analysis. MK performed the statistical analysis, analysed the data, and wrote the manuscript draft. ER, C-OO, and MC contributed to the original concept of the project and supervised the study. All authors contributed to the manuscript and approved the submitted version.

Declaration of generative AI and AI-assisted technologies in the writing process

During the preparation of this work the author(s) used GPT-4 to improve language and readability. After using this tool, the author(s) reviewed and edited the content as needed and take(s) full responsibility for the content of the publication.

Funding

This work was funded by the VALPRO Path, a cofounded Horizon Europe project (grant ID: 10.3030/101059824).

Declaration of competing interest

The authors declare that they have no known competing financial interests or personal relationships that could have appeared to influence the work reported in this paper.

Acknowledgements

We would like to acknowledge the efforts of Esben Nedergård Böwes, Thomas Bak-Østerby, and Nagashree N. Akula for their help and expert guidance during the experiment.

Appendix A. Supplementary data

Supplementary data to this article can be found online at https://doi.org/10.1016/j.plaphy.2025.110325.

Data availability

Data will be made available on request.

References

Abdelhakim, L.O.A., Mendanha, T., Palma, C.F.F., Vrobel, O., Štefelová, N., Zeljković, S.Ć., Tarkowski, P., DE Diego, N., Wollenweber, B., Rosenqvist, E., 2022a. Elevated CO2 improves the physiology but not the final yield in spring wheat genotypes subjected to heat and drought stress during anthesis. Front. Plant Sci. 13.

Abdelhakim, L.O.A., Zhou, R., Ottosen, C.-O., 2022b. Physiological responses of plants to combined drought and heat under elevated CO2. Agronomy 12, 2526.

Ahammed, G.J., Xu, W., Liu, A., Chen, S., 2018. COMT1 silencing aggravates heat stress-induced reduction in photosynthesis by decreasing chlorophyll content, photosystem II activity, and electron transport efficiency in tomato. Front. Plant Sci. 9, 998.

Ahmad, M., Sajjad, M., Ullah, A., Zulfiqar, U., Ul-Allah, S., Waraich, E.A., Din, K.U., Siddique, K.H.M., Farooq, M., 2025. From stress to success: strategies for improving heat tolerance in wheat. J. Agron. Crop Sci. 211, e70048.

Ahmad, U., Hassain, M., Arshad, Z., Ayub, B., 2023. Harnessing potential of plant breeding strategies for climate smart agriculture. Trends Biotech Plant Sci 1, 72–83.

Akula, N.N., Abdelhakim, L., Knazovický, M., Ottosen, C.-O., Rosenqvist, E., 2024. Plant responses to co-occurring heat and water deficit stress: a comparative study of tolerance mechanisms in old and modern wheat genotypes. Plant Physiol. Biochem. 210, 108595.

Bauwe, H., 2023. Photorespiration–Rubisco's repair crew. J. Plant Physiol. 280, 153899.

Ben Mariem, S., Soba, D., Zhou, B., Loladze, I., Morales, F., Aranjuelo, I., 2021. Climate change, crop yields, and grain quality of C3 cereals: a meta-analysis of [CO2], temperature, and drought effects. Plants 10, 1052.

Bennetau-Pelissero, C., 2019. Plant Proteins from Legumes. *Bioactive Molecules in Food*. Springer.

Blonder, B.W., Aparecido, L.M.T., Hultine, K.R., Lombardozzi, D., Michaletz, S.T., Posch, B.C., Slot, M., Winter, K., 2023. Plant water use theory should incorporate hypotheses about extreme environments, population ecology, and community ecology. New Phytol. 238, 2271–2283.

Borrell, A.K., Mullet, J.E., George-Jaeggli, B., VAN Oosterom, E.J., Hammer, G.L., Klein, P.E., Jordan, D.R., 2014. Drought adaptation of stay-green sorghum is associated with canopy development, leaf anatomy, root growth, and water uptake. J. Exp. Bot. 65, 6251–6263.

Boyer, J.S., Mclaughlin, J.E., 2007. Functional reversion to identify controlling genes in multigenic responses: analysis of floral abortion. J. Exp. Bot. 58, 267–277.

Carmo-Silva, A.E., Salvucci, M.E., 2012. The temperature response of CO 2 assimilation, photochemical activities and rubisco activation in Camelina sativa, a potential bioenergy crop with limited capacity for acclimation to heat stress. Planta 236, 1433–1445.

Chauhan, J., Prathibha, M., Singh, P., Choyal, P., Mishra, U.N., Saha, D., Kumar, R., Anuragi, H., Pandey, S., Bose, B., 2023. Plant photosynthesis under abiotic stresses: damages, adaptive, and signaling mechanisms. Plant Stress 10, 100296.

Chaves, M.M., Pereira, J.S., Maroco, J., Rodrigues, M.L., Ricardo, C.P.P., Osório, M.L., Carvalho, I., Faria, T., Pinheiro, C., 2002. How plants cope with water stress in the field? Photosynthesis and growth. Ann. Bot. 89, 907.

Chen, P., Lou, G., Wang, Y., Chen, J., Chen, W., Fan, Z., Liu, Q., Sun, B., Mao, X., Yu, H., 2023. The genetic basis of grain protein content in rice by genome-wide association analysis. Mol. Breed. 43, 1.

Chen, Y., Liang, K., Cui, B., Hou, J., Rosenqvist, E., Fang, L., Liu, F., 2025. Incorporating the temperature responses of stomatal and non-stomatal limitations to photosynthesis improves the predictability of the unified stomatal optimization model for wheat under heat stress. Agric. For. Meteorol. 362, 110381.

Chovancek, E., Zivcak, M., Botyanszka, L., Hauptvogel, P., Yang, X., Misheva, S., Hussain, S., Brestic, M., 2019. Transient heat waves May affect the photosynthetic capacity of susceptible wheat genotypes due to insufficient photosystem I photoprotection. Plants 8, 282.

Crafts-Brandner, S., Law, R., 2000. Effect of heat stress on the inhibition and recovery of the ribulose-1, 5-bisphosphate carboxylase/oxygenase activation state. Planta 212, 67–74.

DE Souza, M.A., DE Andrade, L.I.F., Gago, J., Pereira, E.G., 2024. Photoprotective mechanisms and higher photorespiration are key points for iron stress tolerance under heatwaves in rice. Plant Sci. 342, 112031.

Demidchik, V., 2015. Mechanisms of oxidative stress in plants: from classical chemistry to cell biology. Environ. Exp. Bot. 109, 212–228.

Deva, C.R., Urban, M.O., Challinor, A.J., Falloon, P., Svitákova, L., 2020. Enhanced leaf cooling is a pathway to heat tolerance in common bean. Front. Plant Sci. 11, 19.

Devi, P., Awasthi, R., Jha, U., Sharma, K.D., Prasad, P.V., Siddique, K.H., Roorkiwal, M., Nayyar, H., 2023. Understanding the effect of heat stress during seed filling on nutritional composition and seed yield in chickpea (Cicer arietinum L.). Sci. Rep. 13, 15450.

Diao, H., Cernusak, L.A., Saurer, M., Gessler, A., Siegwolf, R.T., Lehmann, M.M., 2024. Uncoupling of stomatal conductance and photosynthesis at high temperatures: mechanistic insights from online stable isotope techniques. New Phytol. 241, 2366–2378.

Dusenge, M.E., Duarte, A.G., Way, D.A., 2019. Plant carbon metabolism and climate change: elevated CO 2 and temperature impacts on photosynthesis, photorespiration and respiration. New Phytol. 221, 32–49.

Eisenhut, M., Roell, M.S., Weber, A.P., 2019. Mechanistic understanding of photorespiration paves the way to a new green revolution. New Phytol. 223, 1762–1769.

Engineer, C.B., Hashimoto-Sugimoto, M., Negi, J., Israelsson-Nordström, M., Azoulay-Shemer, T., Rappel, W.-J., Iba, K., Schroeder, J.I., 2016. CO2 sensing and CO2 regulation of stomatal conductance: advances and open questions. Trends Plant Sci. 21, 16–30.

Fahad, S., Bajwa, A.A., Nazir, U., Anjum, S.A., Farooq, A., Zohaib, A., Sadia, S., Nasim, W., Adkins, S., Saud, S., 2017. Crop production under drought and heat stress: plant responses and management options. Front. Plant Sci. 1147.

Farooq, M., Hussain, M., Usman, M., Farooq, S., Alghamdi, S.S., Siddique, K.H., 2018. Impact of abiotic stresses on grain composition and quality in food legumes. J. Agric. Food Chem. 66, 8887–8897.

Farooq, M., Nadeem, F., Gogoi, N., Ullah, A., Alghamdi, S.S., Nayyar, H., Siddique, K.H., 2017. Heat stress in grain legumes during reproductive and grain-filling phases. Crop Pasture Sci. 68, 985–1005.

Ferreira, H., Pinto, E., Vasconcelos, M.W., 2021. Legumes as a cornerstone of the transition toward more sustainable agri-food systems and diets in Europe. Front. Sustain. Food Syst. 5, 694121.

Frick, K.M., Foley, R.C., Kamphuis, L.G., Siddique, K.H., Garg, G., Singh, K.B., 2018. Characterization of the genetic factors affecting quinolizidine alkaloid biosynthesis and its response to abiotic stress in narrow-leafed lupin (*Lupinus angustifolius L.*). Plant Cell Environ. 41, 2155–2168.

Hatfield, J.L., Dold, C., 2019. Water-use efficiency: advances and challenges in a changing climate. Front. Plant Sci. 10, 103.

Ibrahim, H.M., 2011. Heat stress in food legumes: evaluation of membrane thermostability methodology and use of infra-red thermometry. Euphytica 180, 99–105.

Jansen, G., Jürgens, H.U., Ordon, F., 2009. Effects of temperature on the alkaloid content of seeds of *Lupinus angustifolius* cultivars. J. Agron. Crop Sci. 195, 172–177.

Jordan, D.B., Ogren, W.L., 1984. The CO2/O2 specificity of ribulose 1,5-bisphosphate carboxylase/oxygenase. Planta 161, 308–313.

Keuleyan, E., Gélébart, P., Beaumal, V., Kermarrec, A., Ribourg-Birault, L., LE Gall, S., Meynier, A., Riaublanc, A., Berton-Carabin, C., 2023. Pea and lupin protein ingredients: new insights into endogenous lipids and the key effect of high-pressure homogenization on their aqueous suspensions. Food Hydrocoll. 141, 108671.

Khanzada, A., Yan, K., Hu, W., Malko, M., Khan, K.A., Bao, Y., Elboughdiri, N., Li, Y., 2025. Heat stress response mechanisms and resilience strategies in wheat. J. Agron. Crop Sci. 211, e70023.

Liu, H., Able, A.J., Able, J.A., 2022. Priming crops for the future: rewiring stress memory. Trends Plant Sci. 27, 699–716.

Luan, X., Vico, G., 2021. Canopy temperature and heat stress are increased by compound high air temperature and water stress and reduced by Irrigation–A modeling analysis. Hydrol. Earth Syst. Sci. 25, 1411–1423.

Lucas, M.M., Stoddard, F.L., Annicchiarico, P., Frías, J., Martínez-Villaluenga, C., Sussmann, D., Duranti, M., Seger, A., Zander, P.M., Pueyo, J.J., 2015. The future of lupin as a protein crop in Europe. Front. Plant Sci. 6, 705.

Mahalingam, R., 2014. Combined Stresses in Plants: Physiological, Molecular, and Biochemical Aspects. Springer.

Mathur, S., Agrawal, D., Jajoo, A., 2014. Photosynthesis: response to high temperature stress. J. Photochem. Photobiol. B Biol. 137, 116–126.

Maxwell, K., Johnson, G.N., 2000. Chlorophyll Fluorescence—A practical guide. J. Exp. Bot. 51, 659–668.

Moore, C.E., Meacham-Hensold, K., Lemonnier, P., Slattery, R.A., Benjamin, C., Bernacchi, C.J., Lawson, T., Cavanagh, A.P., 2021. The effect of increasing temperature on crop photosynthesis: from enzymes to ecosystems. J. Exp. Bot. 72, 2822–2844.

Murchie, E.H., Lawson, T., 2013. Chlorophyll fluorescence analysis: a guide to good practice and understanding some new applications. J. Exp. Bot. 64, 3983–3998.

Pixley, K.V., Cairns, J.E., Lopez-Ridaura, S., Ojiewo, C.O., Dawud, M.A., Drabo, I., Mindaye, T., Nebie, B., Asea, G., Das, B., 2023. Redesigning crop varieties to win the race between climate change and food security. Mol. Plant 16, 1590–1611.

Plaut, Z., Butow, B., Blumenthal, C., Wrigley, C., 2004. Transport of dry matter into developing wheat kernels and its contribution to grain yield under post-anthesis water deficit and elevated temperature. Field Crops Res. 86, 185–198.

Poudyal, D., Rosenqvist, E., Ottosen, C.-O., 2018. Phenotyping from lab to field–tomato lines screened for heat stress using Fv/Fm maintain high fruit yield during thermal stress in the field. Funct. Plant Biol. 46, 44–55.
Proietti, S., Paradiso, R., Moscatello, S., Saccardo, F., Battistelli, A., 2023. Light intensity affects the assimilation rate and carbohydrates partitioning in spinach grown in a controlled environment. Plants 12, 804.
Provera, I., Martinez, M., Zenone, A., Giacalone, V., D'Anna, G., Badalamenti, F., Marín-Guirao, L., Procaccini, G., 2024. Exploring priming strategies to improve stress resilience of Posidonia oceanica seedlings. Mar. Pollut. Bull. 200, 116057.
Raza, A., Bashir, S., Khare, T., Karikari, B., Copeland, R.G., Jamla, M., Abbas, S., Charagh, S., Nayak, S.N., Djalovic, I., 2024. Temperature-smart plants: a new horizon with omics-driven plant breeding. Physiol. Plantarum 176, e14188.
Roman, L., Tsochatzis, E., Tarin, K., Röndahl, E.M., Ottosen, C.O., Corredig, M., 2023. Compositional attributes of blue lupin (Lupinus angustifolius) seeds for selection of high-protein cultivars. Journal of Agricultural and Food Chemistry 71 (45), 17308–17320.
Rosenqvist, E., 2022. Using Phenotyping Techniques to Analyse Crop Functionality and Photosynthesis.
Rotundo, J.L., Westgate, M.E., 2009. Meta-analysis of environmental effects on soybean seed composition. Field Crops Res. 110, 147–156.
Sarkar, S., Khatun, M., Era, F.M., Islam, A., Anwar, M., Danish, S., Datta, R., Islam, A., 2021. Abiotic stresses: alteration of composition and grain quality in food legumes. Agronomy 11, 2238.
Sarto, M.V.M., Sarto, J.R.W., Rampim, L., Rosset, J.S., Bassegio, D., Da Costa, P.F., Inagaki, A.M., 2017. Wheat phenology and yield under drought: a review. Aust. J. Crop. Sci. 11, 941–946.
Sato, H., Mizoi, J., Shinozaki, K., Yamaguchi-Shinozaki, K., 2024. Complex plant responses to drought and heat stress under climate change. Plant J. 117, 1873–1892.
Scafaro, A.P., Posch, B.C., Evans, J.R., Farquhar, G.D., Atkin, O.K., 2023. Rubisco deactivation and chloroplast electron transport rates co-limit photosynthesis above optimal leaf temperature in terrestrial plants. Nat. Commun. 14, 2820.
Sehgal, A., Sita, K., Siddique, K.H., Kumar, R., Bhogireddy, S., Varshney, R.K., Hanumantharao, B., Nair, R.M., Prasad, P.V., Nayyar, H., 2018. Drought Or/And heat-stress effects on seed filling in food crops: impacts on functional biochemistry, seed yields, and nutritional quality. Front. Plant Sci. 9, 1705.
Sharma, D.K., Andersen, S.B., Ottosen, C.O., Rosenqvist, E., 2015. Wheat cultivars selected for high Fv/Fm under heat stress maintain high photosynthesis, total chlorophyll, stomatal conductance, transpiration and dry matter. Physiol. Plantarum 153, 284–298.
Sharma, D.K., Torp, A.M., Rosenqvist, E., Ottosen, C.-O., Andersen, S.B., 2017. QTLs and potential candidate genes for heat stress tolerance identified from the mapping populations specifically segregating for F v/F m in wheat. Front. Plant Sci. 8, 1668.
Siebert, S., Webber, H., Zhao, G., Ewert, F., 2017. Heat stress is overestimated in climate impact studies for irrigated agriculture. Environ. Res. Lett. 12, 054023.
Sita, K., Sehgal, A., Bhandari, K., Kumar, J., Kumar, S., Singh, S., Siddique, K.H., Nayyar, H., 2018. Impact of heat stress during seed filling on seed quality and seed yield in lentil (lens culinaris medikus) genotypes. J. Sci. Food Agric. 98, 5134–5141.
Sita, K., Sehgal, A., Hanumantharao, B., Nair, R.M., Vara Prasad, P., Kumar, S., Gaur, P. M., Farooq, M., Siddique, K.H., Varshney, R.K., 2017. Food legumes and rising temperatures: effects, adaptive functional mechanisms specific to reproductive growth stage and strategies to improve heat tolerance. Front. Plant Sci. 8, 1658.
Sommer, S.G., Li, X., Rosenqvist, E., Liu, F., 2024. Leaf photosynthetic performance is not a key factor affecting grain yield in spring wheat subjected to heat and combined heat and drought stresses. J. Agron. Crop Sci. 210, e12685.
Stanfield, R.C., Bartlett, M.K., 2022. Coordination between phloem loading and structure maintains carbon transport under drought. Front. Plant Sci. 13, 787837.
Sumesh, K., Sharma-Natu, P., Ghildiyal, M., 2008. Starch synthase activity and heat shock protein in relation to thermal tolerance of developing wheat grains. Biol. Plantarum 52, 749–753.
Taria, S., Arora, A., Krishna, H., Manjunath, K.K., Kumar, S., Singh, B., Meena, S., Malakondaiah, A.C., Kousalya, S., Padaria, J.C., 2025. Mapping of the QTLs governing stem-specific weight for stem reserve mobilisation in wheat (Triticum aestivum L.) under combined heat and drought stress. Plant Physiology Reports 1–15.
Timm, S., Hagemann, M., 2020. Photorespiration—How is it regulated and how does it regulate overall plant metabolism? J. Exp. Bot. 71, 3955–3965.
Tugizimana, F., Mhlongo, M.I., Piater, L.A., Dubery, I.A., 2018. Metabolomics in plant priming research: the way forward? Int. J. Mol. Sci. 19, 1759.
Urban, J., Ingwers, M.W., Mcguire, M.A., Teskey, R.O., 2017. Increase in leaf temperature opens stomata and decouples net photosynthesis from stomatal conductance in Pinus taeda and Populus deltoides x nigra. J. Exp. Bot. 68, 1757–1767.
Vadez, V., Berger, J.D., Warkentin, T., Asseng, S., Ratnakumar, P., Rao, K., Gaur, P.M., Munier-Jolain, N., Larmure, A., Voisin, A.-S., 2012. Adaptation of grain legumes to climate change: a review. Agron. Sustain. Dev. 32, 31–44.
Vadez, V., Ratnakumar, P., 2016. High transpiration efficiency increases pod yield under intermittent drought in dry and hot atmospheric conditions but less so under wetter and cooler conditions in groundnut (Arachis hypogaea (L.)). Field Crops Res. 193, 16–23.
Valentini, R., Epron, D., DE Angelis, P., Matteucci, G., Dreyer, E., 1995. In situ estimation of net CO2 assimilation, photosynthetic electron flow and photorespiration in Turkey oak (Q. Cerris L.) leaves: diurnal cycles under different levels of water supply. Plant Cell Environ. 18, 631–640.
Vishnyakova, M., Vlasova, E., Egorova, G., 2021. Genetic resources of narrow-leaved lupine (*Lupinus angustifolius L.*) and their role in its domestication and breeding. Vavilov Journal of Genetics and Breeding 25, 620.
Voss, I., Sunil, B., Scheibe, R., Raghavendra, A., 2013. Emerging concept for the role of photorespiration as an important part of abiotic stress response. Plant Biol. 15, 713–722.
Willett, W., Rockström, J., Loken, B., Springmann, M., Lang, T., Vermeulen, S., Garnett, T., Tilman, D., Declerck, F., Wood, A., 2019. Food in the anthropocene: the EAT–lancet commission on healthy diets from sustainable food systems. Lancet 393, 447–492.
Williams, J.L., Sherman, J.D., Lamb, P., Cook, J., Lachowiec, J.A., Bourgault, M., 2022. Relationships between roots, the stay-green phenotype, and agronomic performance in barley and wheat grown in semi-arid conditions. The Plant Phenome Journal 5, e220050.
Wingler, A., Lea, P.J., Quick, W.P., Leegood, R.C., 2000. Photorespiration: metabolic pathways and their role in stress protection. Philos. Trans. R. Soc. Lond. Ser. B Biol. Sci. 355, 1517–1529.
Woodruff, D.R., 2014. The impacts of water stress on phloem transport in Douglas-fir trees. Tree Physiol. 34, 5–14.
Yang, H., Gu, X., Ding, M., Lu, W., Lu, D., 2018. Heat stress during grain filling affects activities of enzymes involved in grain protein and starch synthesis in waxy maize. Sci. Rep. 8, 15665.
Yang, J., Zhang, J., Wang, Z., Xu, G., Zhu, Q., 2004. Activities of key enzymes in sucrose-to-starch conversion in wheat grains subjected to water deficit during grain filling. Plant Physiol. 135, 1621–1629.
Zhang, W., Boateng, I., Xu, J., Zhang, Y., 2024. Proteins from legumes, cereals, and pseudo-cereals: composition, modification, bioactivities, and applications. Foods 13 (13), 1974.
Zhongming, Z., Linong, L., Xiaona, Y., Wangqiang, Z., Wei, L., 2022. AR6 Synthesis Report: Climate Change 2022.
Zhou, R., Hyldgaard, B., Yu, X., Rosenqvist, E., Ugarte, R.M., Yu, S., Wu, Z., Ottosen, C.-O., Zhao, T., 2018. Phenotyping of faba beans (Vicia faba L.) under cold and heat stresses using chlorophyll fluorescence. Euphytica 214, 1–13.
Zhou, R., Kjær, K.H., Rosenqvist, E., Yu, X., Wu, Z., Ottosen, C.O., 2017. Physiological response to heat stress during seedling and anthesis stage in tomato genotypes differing in heat tolerance. J. Agron. Crop Sci. 203, 68–80.